NTNU
Innovation and Creativity

Radio Resource Allocation for Increased Capacity in Cellular Networks

Sigbjørn Hernes Dybdahl

Master of Science in Communication Technology
Submission date: June 2007
Supervisor: Geir Egil Øien, IET
Co-supervisor: Anders Gjendemsjø, IET

Norwegian University of Science and Technology
Department of Electronics and Telecommunications

Problem Description

Recent research work shows that the total sum network capacity in a cellular network can be increased by alternative cell power allocation policies, instead of letting all cells transmit at full power all the time as is used today. In particular, simple binary power allocation, in which the power in a cell can be adaptively switched on and off during certain time slots (depending on the trade-off between the contribution it gives respectively to the capacity increase and to the overall interference in the network) can give an overall increase in sum capacity.

The goal of this master thesis is (after getting acquainted with the necessary theory to understand the problem) to simulate and analyze various power control and scheduling schemes that seek to maximize the network capacity, with the most emphasis on a thorough understanding of the special case of two-cell networks, under per-base station peak and minimum power constraints. In particular one seeks to understand the influence of a nonzero minimum power constraint.

The simulations are to be based on an existing simulation tool for cellular networks, on which the student can develop his own extensions. The above-mentioned setting opens for many interesting problems, and the student can approach them either by analytical evaluations, computer simulations, or both.

Assignment given: 19. January 2007
Supervisor: Geir Egil Øien, IET

Abstract

Cellular networks are widely deployed for wireless communication, and as the number of users of these networks increase, so does the need for higher spectral efficiency. Clever measures have to be taken in order to increase throughput for wireless networks because of the scarcity of radio resources. Ever higher rates are demanded, but we also want to conserve a fair distribution of the available resources. Therefore, we consider the problem of joint power allocation and user scheduling, while achieving a desired level of fairness in wireless cellular systems. Dynamic resource allocation is employed for the full reuse networks simulated, in order to cope with inter-cell interference and to optimize spectrum efficiency. Binary power allocation is implemented and compared to the performance without power control, for minimum transmit power levels equal to 0 and greater than 0. We show that binary power control with individual power levels for each cell is optimal for two-cell networks. We also present an extension to the proportional fair scheduling for multi-cell networks, and analyze its performance for different cell sizes and time windows. Finally, we highlight the equality between multi-cell, multi-user and multi-carrier proportional fair scheduling. Simulation results show how power control and user scheduling increase throughput, reduce power consumption and achieve a desired level of fairness. Hence, we can obtain considerable gains for the network throughput through adaptive power allocation and multiuser diversity.

Preface

This is the report for my master's thesis which concludes my 10th semester, and my five years as student at the program for communication technology at the Norwegian University of Science and Technology (NTNU), Trondheim, Norway. This master's thesis is the first major, long-term project I have done on my own, and has given me an idea of what research and development in a university context would be like.

This project has been most instructive, especially since I started this master's thesis from scratch and an important part of it has been devoted to understanding the theoretic background. The work has further improved my understanding of cellular networks and their optimization, based on my previous knowledge from courses I have attended. It has been a continuous learning process and I have acquired a new understanding of the challenges associated with wireless communications, power allocation and user scheduling through taking one step at the time, being accurate and constantly verifying obtained results.

I would like to thank Prof. Geir Øien and Anders Gjendemsjø for their continuous guiding and inspiration throughout this period. I would also like to thank Eivind Syvertsen for his thorough introduction to the simulation framework used for this report. My thanks also go out to Hans Jørgen Bang and Marios Kountouris for their help and ideas on scheduling. Finally, I would like to thank my family and friends for the liberty and support, and for making these five years in Trondheim a very memorable experience.

Sigbjørn H. Dybdahl
Trondheim, June 15, 2007

Contents

List of Figures

List of Tables

List of Abbreviations

AWGN	Additive White Gaussian Noise
BPC	Binary Power Control
BS	Base Station
CDMA	Code Division Multiple Access
COST	European Co-operation in the Field of Scientific and Technical Research
COST-WI	COST Action 231 Walfisch-Ikegami model
CSI	Channel State Information
FDMA	Frequency Division Multiple Access
GP	Geometric Programming
GSM	Global System for Mobile Communications
JFI	Jain's fairness index
LOS	Line of Sight
M-PFS	Multi-cell Proportional Fair Scheduling
Max-Cap	Maximum Capacity Scheduling
Max-SNR	Maximum SNR Scheduling
NP-hard	Non-deterministic Polynomial-time hard
PDF	Probability Density Function
PFS	Proportional Fair Scheduling
QoS	Quality of Service

RR	Round Robin Scheduling
SNIR	Signal to Noise-plus-Interference Ratio
SNR	Signal to Noise Ratio
TDMA	Time Division Multiple Access
UT	User Terminal
V-PFS	Vectorized Proportional Fair Scheduling
WI-LOS	Walfisch-Ikegami Line of Sight model

Chapter 1

Introduction

Cellular networks are widely adopted and have become a familiar term for most of us. As these networks have become very popular, the demand for higher capacity follows naturally. That is, more users and new services require networks with greater throughput. Given the nature of the wireless channel, clever measures have to be taken to achieve higher spectrum efficiency since the spectral resources are scarce.

Higher spectrum efficiency requires system-wide optimization of the resources [24]. Accordingly, in order to achieve an increased throughput, we need to consider a global approach to the problem, and look at the network as a whole. By applying the principle of full resource reuse in combination with dynamic resource allocation in the considered network, we can better exploit the limited resources available. As full resource reuse means higher interference levels from neighbouring cells, since they are using the same spectrum resources, dynamic resource allocation is necessary to control inter-cell interference. In contrast, static resource allocation, as seen in current cellular networks with disjoint resource use in neighbouring cells, does not take into consideration the actual propagation channel by assigning the same resources regardless of the channel conditions.

In this report we consider the problem of simultaneous optimization of transmission rates and power control, and of how we can achieve a desired degree of fairness through centralized algorithms. The problem of balancing system throughput while serving users in a fair manner in a network-wide context with proportional fairness is NP-hard [17]. As a result, the problem has not been given high priority until now, but it has recently received an increase in interest [3, 22, 24, 25]. Having cells, users, power levels and scheduling as degrees of freedom, it is clear that centralized control is complex with the need for synchronization and channel state information processing [21], which is particularly difficult in an environment with rapidly changing channel conditions.

This master's thesis has been a study of the behaviour of different scheduling and power allocation algorithms based on the results from simulations done in Matlab from Mathworks, based on a framework made by PhD student Anders Gjendemsjø. The simulations benefit from the advances made through the introduction of binary power control in reducing optimization complexity in our quest to increase spectrum efficiency and achieve desired fairness.

The traffic in cellular networks is by now considered to be data-centric, and no longer voice-centric as was the case in the beginning. We also assume that we can employ adaptive coding and modulation, varying the user rates instantaneously according to the channel characteristics. For this type of wireless data access network, we use the total system throughput as a measure of system performance since in general there is a significant demand for high data rates.

The main priority for this master's thesis has been to investigate the possibilities to improve fairness in networks with binary power allocation, as well as getting insight in the problem in order to ease the task of finding distributed algorithms that have the same characteristics. Two main directions have been considered for the analysis of fairness in this report: through an increase of the minimum transmit power level to guarantee transmission for all users, and by using scheduling algorithms that provide a high level of fairness.

The simulations have been performed on two-cell or small multicell networks allowing for in depth studies. The results presented here carry over to larger networks for example by clustering, and leads the way in finding algorithms that achieves throughputs close to optimal performance, but with a significant drop in complexity.

The remainder of the report is organized as follows:

Chapter 2 describes fundamentals for wireless communications, such as signal propagation, fading and shadowing.

Chapter 3 presents the interest in using power control and scheduling, and the combination of both through joint power allocation and scheduling.

Chapter 4 treats the implementational choices and issues in the simulation framework.

Chapter 5 presents the achieved simulation results for different scenarios.

Chapter 6 analyzes and discusses the findings.

Chapter 7 gives the conclusions of the report and presents topics for future work.

Chapter 2

Wireless communication fundamentals

Wireless transmission is a difficult task since we are forced to use an unpredictable channel for reliable communication. The unpredictability lies in that the channel changes in time and with position because electromagnetic waves propagate through environments where they are reflected, diffracted and absorbed. In other words, the received signal may differ from the transmitted signal in both strength and information caused by noise and amplitude and phase changes during propagation.

In [7] it is explained that path loss is the dissipation of power from the transmitter and effects of the propagation channel on the signal, and that shadowing is the attenuation of the signal amplitude caused by obstacles between the transmitter and the receiver. Thus, path loss and shadowing are called large-scale propagation effects since they occur over larger distances (between 10 and 1000 meters). Small-scale propagation effects occur over distances comparable to the signal wavelength, including multipath fading, which is caused by constructive and destructive addition of multipath signal components due to phase variations.

To know the entire distribution of waves for a given propagation environment, the equations of James Clerk Maxwell have to be solved. Therefore, approximations to Maxwell's equations are used, since these calculations do not require the knowledge of every parameter in question. But as the complexity increases, it is difficult to achieve an accurate deterministic model. Hence, an empirical model based on simulation results in various environments would be more appropriate, which is explained in the following sections.

2.1 Path loss

Generally speaking, the path loss is the ratio between transmitted power P_t and received power P_r for, respectively, the transmit and the receive antennas:

$$PL \text{ dB} = 10 \log_{10} \frac{P_t}{P_r} \text{ dB} \tag{2.1}$$

which in dB is a nonnegative number since the channel only attenuates the signal. We can also talk about the path gain, which in dB is the negative of the path loss, i.e., PG dB $= -PL$ dB.

Several different approaches are possible when it comes to describing the path loss, and the following subsections describe two of them.

2.1.1 Free-space path loss

This is simplest path loss model which is based on a signal transmitted a distance d with no obstructions between the transmitter and receiver. This is known as a line-of-sight (LOS) model since the signal experiences no obstructions between the transmitter and receiver antennas. The free-space path loss is described by following equation:

$$PL \text{ dB} = 10 \log_{10} \frac{P_t}{P_r} = -10 \log_{10} \frac{G_{i,i}\lambda^2}{(4\pi d)^2} \tag{2.2}$$

where $G_{i,i}$ is the channel gain, λ is the signal wavelength, and d is the propagation distance. Thus, the received power decreases at the rate of the square of the distance d.

The free-space path loss model can be extended by using the technique of ray-tracing. That is, reflected, diffracted or scattered components of the signal are included in the model, in addition to the LOS component. This requires more knowledge of the propagation environment, such as buildings and their location and dielectric coefficients. If the number, location and characteristics of reflectors is not known over time, statistical models must be used [7].

2.1.2 Empirical based path loss

A different approach is based on using empirical models founded on measurements instead of geometrical or statistical models. Since most mobile communication systems operate in complex propagation environments that cannot be accurately modelled by free-space path loss or ray-tracing, several models have been developed to predict path loss based on measurements for a given distance and frequency in a geographical area [7]. The empirical models can be adapted for a suitable environment with a set of parameters.

The framework for European Co-operation in the Field of Scientific and Technical Research (COST) is a large, intergovernmental organization for research on a European level, and its report for COST Action 231 [1] proposes several models based on the approaches of Hata and Walfisch-Ikegami, with some differences when it comes to their restrictions for the parameters.

- The COST-Hata model is the COST 231 extension to Hata's model, where the

path loss is given by:

$$PL \text{ dB} = 46.3 + 33.9 \log_{10} \frac{f}{\text{MHz}} - 13.82 \log_{10} \frac{h_b}{\text{m}} - a(h_m) + \left(44.9 - 6.55 \log_{10} \frac{h_b}{\text{m}}\right) \log_{10} \frac{d}{\text{km}} + C_m \tag{2.3}$$

$$\text{where } a(h_m) = \left(1.1 \log_{10} \frac{f}{\text{MHz}} - 0.7\right) \frac{h_m}{\text{m}} - \left(1.56 \log_{10} \frac{f}{\text{MHz}} - 0.8\right), \tag{2.4}$$

and is restricted to the following range of parameters:

$$\begin{aligned} f &\in [1500, 2000] \text{ MHz} \\ h_b &\in [30, 200] \text{ m} \\ h_m &\in [1, 10] \text{ m} \\ d &\in [1, 20] \text{ km} \\ C_m &= \begin{cases} 0 \text{ dB} & \text{for medium sized cities and suburbs} \\ 3 \text{ dB} & \text{for metropolitan areas} \end{cases} \end{aligned}$$

- The COST-Walfisch-Ikegami model is the proposed combination of Walfisch's and Ikegami's models, which exists in two different editions; with and without LOS components. For the LOS case, the model is given by [1]:

$$PL \text{ dB} = 42.6 + 26 \log_{10} \frac{d}{\text{km}} + 20 \log_{10} \frac{f}{\text{MHz}} \tag{2.5}$$

and is restricted to the following range of parameters:

$$\begin{aligned} f &\in [800, 2000] \text{ MHz} \\ h_b &\in [4, 50] \text{ m} \\ h_m &\in [1, 3] \text{ m} \\ d &\in [0.02, 5] \text{ km} \end{aligned}$$

We see that the models have different operating ranges regarding operating frequency f, base station height h_b, mobil user terminal height h_m and distance d between BS and UTs. Whereas the COST-Hata model is restricted to macro-scale cells, the COST-Walfisch-Ikegami model can be applied to micro-cells with users at a distance $d = 20$ m from the base station.

2.2 Shadowing

As mentioned in the beginning of Section 2, shadowing is the attenuation of the signal caused by obstacles in the propagation path. These obstacles give rise to random

variations in the received signal power at a given distance, since the position and characteristics of reflecting surfaces and scattering objects may change. A common model for this additional attenuation is log-normal shadowing, given by [7]:

$$p(\psi) = \frac{\xi}{\sqrt{2\pi}\sigma_{\psi_{\mathrm{dB}}}} \exp\left(-\frac{10\ \log_{10}\psi - \mu_{\psi_{\mathrm{dB}}}}{2\sigma^2_{\psi_{\mathrm{dB}}}}\right), \psi > 0 \tag{2.6}$$

where $\xi = 10/\ln 10$, $\mu_{\psi_{\mathrm{dB}}}$ is the mean of $\psi_{\mathrm{dB}} = 10\ \log_{10}\psi$ in decibels, and $\sigma_{\psi_{\mathrm{dB}}}$ is the standard deviation of ψ_{dB} in decibels. Thus, the log-normal distribution is defined by two parameters $\mu_{\psi_{\mathrm{dB}}}$ and $\sigma_{\psi_{\mathrm{dB}}}$, which can be based on an analytical model or on empirical measurements.

2.3 Multipath fading

Multipath fading was defined earlier in Section 2 as the result of constructive and destructive addition of multipath signal components. The distribution of the multipath fading depends on the model used for the propagation channel. That is, we can choose between models incorporating a LOS component, and models without a LOS component for the multipath fading distribution.

We consider $b_{\mathrm{I}}(t)$ and $b_{\mathrm{Q}}(t)$, the in-phase and the quadrature components, respectively, of the received signal, and we have the following relationship between them:

$$\phi = |b(t)| = \sqrt{b^2_{\mathrm{I}}(t) + b^2_{\mathrm{Q}}(t)}\,, \tag{2.7}$$

where ϕ is the signal envelope, and $b(t)$ is the received signal. For the development of the probability density function (PDF) for the two following scenarios, we consider two Gaussian random variables B_{I} and B_{Q}, and their relationship $\Phi = \sqrt{B^2_{\mathrm{I}} + B^2_{\mathrm{Q}}}$.

- Without a LOS component, B_{I} and B_{Q} have zero mean and equal variances, and the signal amplitude is Rayleigh distributed with the following PDF [7]:

$$p_{\Phi}(\phi) = \frac{\phi}{\sigma^2} \exp\left(-\frac{\phi^2}{2\sigma^2}\right), \phi \geq 0\,. \tag{2.8}$$

  This makes the received signal power exponentially distributed with mean $2\sigma^2$ by making the change of variables $\xi = \phi^2 = |b(t)|^2$, or:

$$p_{\Phi^2}(\xi) = \frac{1}{2\sigma^2} \exp\left(-\frac{\xi}{2\sigma^2}\right)\,. \tag{2.9}$$

- With a LOS component, B_{I} and B_{Q} no longer have zero mean since we have a superposition of a a complex Gaussian component and a LOS component. The signal can be shown to be Rician distributed with PDF expressed by:

$$p_{\Phi}(\phi) = \frac{\phi}{\sigma^2} \exp\left(\frac{-\left(\phi^2 + s^2\right)}{2\sigma^2}\right) I_0\left(\frac{\phi s}{\sigma^2}\right), \phi \geq 0\,, \tag{2.10}$$

where $2\sigma^2$ is the average power in the non-LOS components, and s^2 is the power in the LOS component. The function I_0 is a modified Bessel function of first kind and zeroth order, defined by:

$$I_0(x) = \frac{1}{2\pi} \int_{-\pi}^{\pi} e^{x \cos\theta} \mathrm{d}\theta \ . \tag{2.11}$$

The Rician K factor is defined as the ratio of signal power in the LOS component over the scattered, reflected power, or $K = s^2/2\sigma^2$ [16]. The parameter is often used when describing the fading introduced by a Rician distributed multipath fading. We note that when $K = 0$, we have no LOS component, and Rician distributed fading is equivalent with Rayleigh distributed fading. When $K = \infty$, we have only a LOS component and there is no multipath fading. K is therefore a measure of the severity of the fading: a small K implies severe fading, a large K implies relatively mild fading [7].

Using K and $\bar{P}_r = s^2 + 2\sigma^2$, the total local-mean power, we can rewrite (2.10) according to [7, 16] on the following form:

$$p_\Phi(\phi) = \frac{2\phi(1+K)}{\bar{P}_r} \exp\left(-K - \frac{(1+K)\phi^2}{\bar{P}_r}\right) I_0\left(2\phi\sqrt{\frac{2K(1+K)}{\bar{P}_r}}\right) \ . \tag{2.12}$$

From (2.12) and making the same change of variables as for (2.9), we have the following expression for the probability distribution function for the received signal power:

$$p_{\Phi^2}(\xi) = \frac{1+K}{\bar{P}_r} \exp\left(-K - \frac{(1+K)\xi}{\bar{P}_r}\right) I_0\left(2\sqrt{\frac{2K(1+K)\xi}{\bar{P}_r}}\right) \ . \tag{2.13}$$

This concludes the introduction to parts of the fundamental theory on wireless communications, and we will in the following chapter present techniques to improve capacity and fairness through power allocation and scheduling. The effects and models described so far will be put to use when analyzing and assessing these techniques.

Chapter 3

Power allocation and scheduling

Current cellular networks employ some form for power allocation and user scheduling in order to decide which users are to receive information at a given moment. Based on the goal of achieving higher spectrum efficiency and a desired level of fairness in resource distribution, we will present in the following sections strategies for power allocation, scheduling, and joint power allocation and scheduling.

3.1 System model

We consider a multi-cell network with N neighbouring cells, and U mobile user terminals (UTs) within the coverage area of each base station (BS). A possible realization of this setup is illustrated in Figure 3.1.

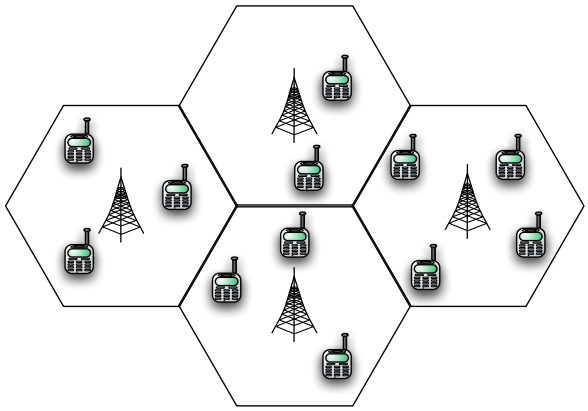

Figure 3.1: Sample network setup.

Our model is limited to downlink transmission, but the results can be generalized

to uplink. For a given (spectral) resource slot, where resource slots can be time in Time division multiple access (TDMA), frequency in Frequency division multiple access (FDMA) or code in (orthogonal) Code division multiple access (CDMA), a single user is supported in each cell. We have a full reuse network setup, which means that all system resources are shared between all cells, leading to an interference and noise impaired system since all users will experience interference from neighbouring cells [21].

In an attempt to better exploit the system resources, we apply power control on the BS's, with the following minimum and peak power constraints:

$$P_{\text{min,i}} \leq P_i \leq P_{\text{max,i}}\,,\ \forall i \in \{1,\ldots,N\}\,. \tag{3.1}$$

The use of power control also helps reducing inter-cell interference present in cellular networks, as BSs can emit lower power levels, and we can even turn off cells if $P_{\min} = 0$.

The distribution of power to the different cells can be either a centralized or a distributed process. That is, we have to select between having a central unit that knows the channel characteristics in all cells and decides the optimal power level in each cell, or using a distributed algorithm that makes each cell able to decide its transmit power level on its own. Independently of the selected strategy, there is a need for channel state information (CSI) to be sent between UTs and the BS by means of a feedback channel in order to make a decision.

We model the received signal by user i in a given resource slot, under the assumption that the coherence time of the channel is longer than the scheduling period, as:

$$Y_i = \sqrt{G_{i,i}}X_i + \sum_{j\neq i}^{N} \sqrt{G_{i,j}}X_j + Z_i\,, \tag{3.2}$$

where $G_{i,j} \in \mathbb{R}^+$ is the channel gain between user i and base station j, X_j is the signal emitted from BS j, and Z_j is additive white Gaussian noise. Based on (3.2), and $\mathbb{E}[|X_i|^2] = P_i$ and $\mathbb{E}[|Z_i|^2] = \sigma_i^2$ we define the signal to noise-plus-interference ratio (SNIR) as:

$$\text{SNIR}_i = \frac{P_i G_{i,i}}{\sigma_i^2 + \sum_{j\neq i} P_j G_{i,j}}\,. \tag{3.3}$$

3.2 Power allocation

In cellular networks, the power allocation strategy determines the possible throughput for the users in the cells, given the channel characteristics and noise level, as we from information theory know that the capacity is a function of the emitted power and noise [19]. As a result, the SNIR will tell the achievable rate for a user in a cell.

We model the transmission system as an additive white gaussian noise (AWGN) channel, assuming that we emit with gaussian distributed signals in all cells. Hence, the interference will also be gaussian and scaled by the channel gains. The relationship

between the maximal achievable rate and the SNIR is expressed by:

$$R_i = \log_2 (1 + \text{SNIR}_i) = \log_2 \left(1 + \frac{P_i G_{i,i}}{\sigma_i^2 + \sum_{j \neq i} P_j G_{i,j}} \right) , \tag{3.4}$$

where P_i is the emitted power in cell i, $G_{i,i}$ is the direct channel in cell i, $G_{i,j}$ is the interference channel from cell j to cell i and σ_i^2 is the additive noise in cell i.

We define the transmit power vector as:

$$\mathbf{P} = [P_1 \dots P_n \dots P_N] , \tag{3.5}$$

which contains the power levels for all N base stations used to communicate with their respective users. This section will only deal with power allocation for a predetermined set of users, as section 3.3 covers scheduling and section 3.4 covers joint power allocation and scheduling.

The problem of power control in the general SNIR regime proves to be very difficult due to the lack of convexity [3, 21]. That is, standard optimization techniques cannot be applied, which forces us to find alternative techniques to solve the optimization problem. One way of looking at the problem is by considering (restrictions of) the domain of the optimization problem, which is the topic for the three following subsections.

3.2.1 Full power allocation

Full power is the trivial power allocation strategy assuring that all cells are turned on all the time. The other trivial power allocation with all cells turned off is obviously of no interest, since there would be no activity between BTs and UTs.

The strategy of allocating full power to all cells gives the following domain of possible transmit vectors:

$$\Omega_{FP} = \{ \mathbf{P} \mid P_i = P_{\max}, \ \forall i \} ,$$

which we can describe as static power control, since the same transmit power is used for all cells all the time. This is known from many present-day cellular networks. The great advantage is its simplicity, since there is no need for communicating selected power levels between BS's. An inconvenience is that full power allocation introduces a significant level of interference. In order to avoid the unwanted interference, neighbouring network cells may use disjoint frequency resources, as employed in for instance Global System for Mobile Communications (GSM), which results in a fixed cell reuse pattern that is set once and for all.

3.2.2 Continuous power allocation

Continuous power allocation, or dynamic power control, exploits the time varying channel conditions by selecting an appropriate power level in order to maximize capacity at each time slot. The main idea behind adjusting the power levels is to increase capacity through limiting undesirable interference to neighbouring cells, where a reduction in

power consumption can be considered a positive side-effect. An exchange of information about the selected power level at each BS is necessary in order to calculate achievable throughput in the cells, which results in an increase in system complexity.

Having a continuous interval of possible power levels gives the following set of feasible transmit power vectors:

$$\Omega = \{\mathbf{P} \mid P_{\text{min,i}} \leq P_i \leq P_{\text{max,i}},\ \forall i\}\,,$$

where P_{min} and P_{max} are minimum and maximum power, respectively, emitted by the BS.

The introduction of power control means that base stations can be turned off assuming $P_{\text{min}} = 0$ when the channel conditions call for a shutdown of the BS. To rephrase, when a cell contributes less in system capacity than the level of interference it creates for neighbouring cells, we can choose to turn it off. A cell can be turned off during one scheduling period, but may be active the next period.

We note that for $P_{\text{min}} > 0$ cells will not be completely shut down and cells will always emit with a minimum level, but the idea of comparing added throughput and interference remains the same. The reuse pattern obtained with the power control is random, possibly highly irregular, and varies from one scheduling period to the next as a function of the CSI of the cell users [15, 22].

The principle of power control can be carried out either in a centralized or distributed manner. Either way, we want to solve the following optimization problem independently of the way in which power control is done:

$$\begin{aligned} R &= \sum_{i=1}^{N} R_i \\ &\text{s.t. } P_{\text{min,i}} \leq P \leq P_{\text{max,i}}\,, \end{aligned} \tag{3.6}$$

i.e., find

$$\begin{aligned} \mathbf{P}^* &= \underset{\mathbf{P}\in\Omega}{\operatorname{argmax}}\, R = \underset{\mathbf{P}\in\Omega}{\operatorname{argmax}} \sum_{i=1}^{N} R_i \\ &= \underset{\mathbf{P}\in\Omega}{\operatorname{argmax}} \sum_{i=1}^{N} \log_2\left(1 + \frac{P_i G_{i,i}}{\sigma_i^2 + \sum_{j\neq i} P_j G_{i,j}}\right) \\ &= \underset{\mathbf{P}\in\Omega}{\operatorname{argmax}} \log_2 \prod_{i=1}^{N}\left(1 + \frac{P_i G_{i,i}}{\sigma_i^2 + \sum_{j\neq i} P_j G_{i,j}}\right). \end{aligned} \tag{3.7}$$

The optimization problem becomes increasingly complex as each new cell adds a new dimension to the optimization space. Consequently, doing an exhaustive search for all values in Ω to find $\mathbf{P}^*$ rapidly becomes unfeasible for implementation.

3.2.3 Binary power allocation

Binary power allocation is a discretization of the optimization space, which reduces the number of solutions to search over and lowers the feedback rate between network nodes [21]. The main idea behind binary power allocation is to reduce the complexity introduced with dynamic power allocation without sacrificing too much of the optimality achieved with continuous power allocation. This gives the following domain of feasible transmit power vectors:

$$\Delta\Omega = \{\mathbf{P} \mid P_i = P_{\text{min,i}} \text{ or } P_i = P_{\text{max,i}}, \forall i\},$$

where the use of binary[1] comes from the fact that we have two possible values for P_i; either $P_{\text{min,i}}$ or $P_{\text{max,i}}$.

The following two paragraphs will discuss two cases of binary power allocation; first for two-cell networks, followed by the generalized multi-cell network case.

Two-cell case

As already mentioned, binary power allocation introduces a significant reduction in the optimization space for (3.7). More importantly, for two-cell networks, binary power allocation is an optimal power allocation strategy, according to [14, 24, 25]. Thus, the set of feasible power transmit vectors is reduced to $\Delta\Omega = \{(P_{\min}, P_{\max}), (P_{\max}, P_{\min}), (P_{\max}, P_{\max})\}$. We note that $\Delta\Omega$ includes the trivial solution of having all cells switched on, and that the other power transmit pairs are corner points of the optimization space.

The following proposition highlight the results on binary power allocation for two-cell networks.

Proposition 1. *The optimal transmit power allocation for two-cell networks is binary.*

Proof. We have a power domain defined by $\Delta\Omega = \{(P_{\min}, P_{\max}), (P_{\max}, P_{\min}), (P_{\max}, P_{\max})\}$, and we consider [25, Lemma 1] which imply that one cell will transmit with maximum power. Furthermore, [14, 24] show that binary power control is optimal for $P_{\min} = 0$, which is extended in [25] to be valid for any real and non-negative value of $P_{\min}$.

To explain the optimality of binary power allocation for two-cell networks we first check if the emitted power level is an extremal point on the boundary of our optimization domain. That is, we know that one of the cells will be emitting with $P_{\max}$, so we let the transmit power be $(P_1, P_{\max})$, and we see if $\frac{\partial R(P_1, P_{\max})}{\partial P_1} = 0$. Then we check if the value of P_1 is a maximum or minimum for $R(P_1, P_{\max})$ by calculating $\frac{\partial^2 R(P_1, P_{\max})}{\partial P_1^2}$.

[25] show that $\frac{\partial^2 R(P_1, P_{\max})}{\partial P_1^2} > 0$ and that $R(P_1, P_{\max})$ is convex with respect to $P_{\min} \leq P_1 \leq P_{\max}$, which by symmetry holds for P_2 as well. In other words, having a convex function we know that extremal points give the maximal value for the function, and by showing that the expression for the rate is convex, we conclude that the emitted power level is either the minimum or the maximum value. □

[1] In this report we use the notation on/off power allocation when $(P_{\min}, P_{\max}) = (0, 1)$, and binary power allocation otherwise.

Next, we extend Proposition 1 to be valid when individual power constraints are employed in each cell.

Proposition 2. *Binary power allocation with individual power constraints in each cell is optimal for two-cell networks.*

Proof. This is an extension to Proposition 1, where the considered power domain is defined by $\Delta\Omega = \{(P_{\min,1}, P_{\max,2}), (P_{\max,1}, P_{\min,2}), (P_{\max,1}, P_{\max,2})\}$.

First we extend [25, Lemma 1] for individual power constraints. That is, the optimal transmit power vector will have at least one component equal to $P_{\max,\mathrm{i}}$, which satisfies [25, (6)]:

$$R(\alpha\mathbf{P}) = \log_2 \prod_{i=1}^{2} \left(1 + \frac{P_i G_{i,i}}{\frac{\sigma_i^2}{\alpha} + \sum_{j \neq i} P_j G_{i,j}} \right) > R(\mathbf{P}) \,, \text{for}\, \alpha > 1, \mathbf{P} \in \Omega. \tag{3.8}$$

We will follow the same development as for the previous proposition by replacing the unique power levels with the corresponding power level for the cell in question. Since the new power levels also are real and non-negative, the expressions for the derivative and the second derivative of $R(P_1, P_{\max,2})$ remain valid. That is, $\frac{\partial^2 R(P_1, P_{\max,2})}{\partial P_1^2} > 0$ and $R(P_1, P_{\max,2})$ is convex with respect to $P_{\min,1} \leq P_1 \leq P_{\max,1}$, which by symmetry also holds for P_2

Hence, we have a generalization of the optimization space, but it does not alter the results from the proof in proposition 1 as binary power allocation is still optimal for two-cell networks. □

The results from Propositions 1 and 2 regarding the optimization space is illustrated in Figure 3.2, where Figure 3.2a corresponds to $P_{\min,\mathrm{i}} = 0$ and $P_{\max,\mathrm{i}} = P_{\max}$, Figure 3.2b corresponds to $P_{\min,\mathrm{i}} = P_{\min}$ and $P_{\max,\mathrm{i}} = P_{\max}$, and Figure 3.2c corresponds to $P_{\min,1} \neq P_{\min,2}$ and $P_{\max,1} \neq P_{\max,2}$. We note that only the red corner points are in $\Delta\Omega$.

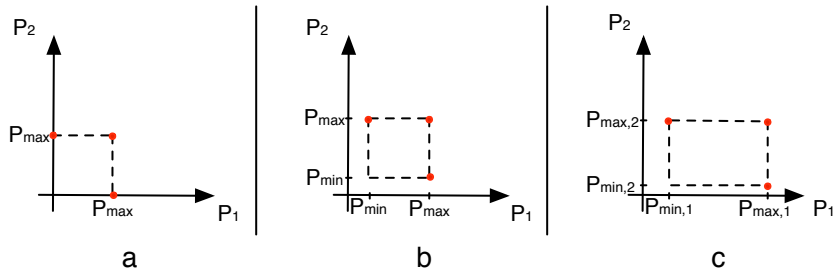

Figure 3.2: Binary power domain $\Delta\Omega$ for various cases.

The previous propositions demonstrate that not only on/off power allocation is optimal, but also binary power allocation with individual power constraints in each cell gives optimal solutions when maximizing the throughput rate in a two-cell network. This

result could be exploited for instance in a two-cell scenario where cell 1 has good channel conditions while cell 2 have poor channel conditions, by allocating more power to cell 2 than cell 1 in order to get equal minimum throughput rates for users in both cells.

Multi-cell case

Motivated by the optimality of binary power allocation for two-cell networks, we increase the number of cells considered in the network and we observe some interesting properties. [25] demonstrate that binary power allocation introduce a negligible loss in achieved throughput, while the reduced optimization space lowers complexity and feedback rate. Thus, binary power allocation no longer is optimal for multi-cell networks, but still yields a performance very close to that obtained by optimally allocating power.

As pointed out by [21], binary power allocation remains exponentially complex in the number of cells, but its discrete nature of power optimization leads the path to simpler, iterative and distributive approaches. That is, the benefits of introducing binary power control overshadows the loss in system capacity, which makes it highly interesting in the search of a higher system ressource efficiency.

The following table summarizes the different power allocation techniques.

Strategy	*Type*	*Domain*	*Characteristic*
Full power	Static	Ω_{FP}	Only 1 point used
Continuous power	Dynamic	Ω	All points considered
Binary power	Dynamic	$\Delta\Omega$	Corner points only

Table 3.1: Power allocation overview

3.3 Scheduling

Multiple scheduling strategies exist which all have their strengths and weaknesses when it comes to complexity, capacity, and fairness. When selecting an algorithm for a cellular network the ideal solution is a scheduling that has low complexity, high capacity, and high fairness, but unfortunately we are forced to make a trade-off between these performance criteria.

When considering fairness for scheduling algorithms, it should be done over a window in time. Scheduling algorithms that obtain high fairness over a relatively short time-window are denoted as short-term fair, while the algorithms that obtain high fairness over an infinite time-window are denoted as asymptotically fair [9]. In addition, we can characterize a scheduling algorithm by the expressions for time-slot fairness and throughput fairness [23] obtained when using Jain's fairness index[2] (JFI) [11].

This section presents different scheduling algorithms, where a selection is used for the simulations in this report. It is interesting to note that the simplest algorithm does

[2]JFI is an index for how time-slots, throughput or other relevant measures are divided among users, and is bounded between 0 and 1, where 0 means total unfairness and 1 means total fairness.

not take into consideration the current channel conditions, while the more sophisticated do take advantage of the varying channels the different users experience, which is also known as multiuser diversity [13].

Generally speaking, as explained in [22], a scheduling algorithm finds the scheduling vector $\mathbf{I}$, where the vector contains the set of scheduled users across all cells:

$$\mathbf{I} = [i_1 \dots i_n \dots i_N].$$

The domain of possible scheduling vectors is given by:

$$\Psi = \{\mathbf{I} \mid 1 \leq i_n \leq U,\ \forall n\},$$

where N is the number of cells and U is the number of users in each cell. We assume that U is equal in all cells, but the results are also valid for a different number of users in each cell.

Combining power allocation and scheduling in a joint process, we want to solve an expression on the following form:

$$(\mathbf{I}^*, \mathbf{P}^*) = \underset{\substack{\mathbf{I}\in\Psi \\ \mathbf{P}\in\Omega}}{\operatorname{argmax}} \mathcal{F}(\mathbf{I}, \mathbf{P}), \tag{3.9}$$

where $\mathcal{F}$ is dependent on the chosen scheduling strategy. As mentioned in [22], this solution is hard to find due to the non-convexity of the problem. Several approaches are possible when attacking this problem, such as minimizing the total transmit power subject to minimum throughput constraints [18], or maximizing the total system throughput [24].

3.3.1 Round Robin Scheduling

Round Robin (RR) is a classic scheduling algorithm assigning users on a turn by turn basis, i.e., the users get a fair share of the system resources by being assigned an equal amount of time slots. This algorithm is simple to implement, and is used in GSM, among others. We note that this algorithm is usually used in each cell seperately, thus not needing any inter-cell communication.

RR scheduling appears in two flavours in this report; with and without power control denoted as (RR-P) and (RR), respectively. The traditional scenario is without power control, that is, each cell emits with full power all the time. As explained in [24], the system capacity can be increased by introducing centralized power control at each time slot by solving (3.7) for each combination of users selected by the Round Robin scheduling.

3.3.2 Maximum SNR Scheduling

Maximum SNR (Max-SNR) scheduling [2] exploits the channel variations in wireless communications by selecting the user that has the highest signal-to-noise ratio (SNR),

seeking to maximize the cell throughput. The algorithm selects a user in a given time slot based on the following expression:

$$i^*(t) = \underset{i \in \Psi}{\operatorname{argmax}} \, \mathrm{SNR}_i = \underset{i \in \psi}{\operatorname{argmax}} \, \frac{G_{i,i}(t)}{\sigma_i^2(t)}, \tag{3.10}$$

where $G_{i,i}(t)$ is the signal strength experienced by user i at time slot t, and $\sigma_i^2(t)$ is the noise experience by user i at time slot t. We note that this algorithm considers cells independently, meaning that it does not take into consideration interference and is only optimal capacity-wise for one-cell networks.

As for Round Robin scheduling, Max-SNR can be improved by applying the principle of centralized power control for all users and cells; thus improving system capacity, but also increasing complexity.

3.3.3 Proportional Fair Scheduling

Proportional Fair Scheduling (PFS), presented in [4, 7, 12], among others, bases the user selection on a metric which takes into consideration both the current rate and the rate achieved over a predetermined time window.

Given the same channel characteristics, equal power and time is given to users who only differ in distance from the BS [12]. Hence, the proportional fair algorithm introduces a notion of fairness when selecting users as opposed to maximizing cell capacity for Max-SNR scheduling.

The algorithm can be expressed as follows:

$$i^*(t) = \underset{k \in \Psi}{\operatorname{argmax}} \, \frac{R_k(t)}{T_k(t)} \tag{3.11}$$

$$T_k(t+1) = \begin{cases} (1 - \frac{1}{i_c})T_k(t) + \frac{1}{i_c}R_k(t) & k = i^*(t) \\ (1 - \frac{1}{i_c})T_k(t) & k \neq i^*(t) \end{cases}, \tag{3.12}$$

where $R_k(t)$ is the rate for user k at instant t, $T_k(t)$ is the average throughput for user k at instant t, and i_c is the predetermined fairness time horizon for the algorithm.

We formally define the requirements for a proportional fair scheduling algorithm in the following definition, which we will use later on to show that a scheduling algorithm indeed is proportional fair.

Definition. *A proportional fair scheduling algorithm should maximize the sum of the logarithmic average user rates over all users [4, 8], i.e. solve:*

$$\mathbf{I}^*(t) = \underset{\mathbf{I} \in \Psi}{\operatorname{argmax}} \sum_k \log T_k(t) \, . \tag{3.13}$$

For a scheduling algorithm based on proportional fairness, the size of i_c determines the importance of the average throughput for a user. That is, a large i_c takes into consideration the throughput achieved by a user over a long time window, whereas a small i_c only consider recent rates. When i_c grows to infinity, we note that PFS is reduced to allocating the system resources to the user with the best channel, i.e. to Max-SNR scheduling, given that all users have the same average SNR [7].

3.4 Joint power allocation and scheduling

In this section, we present two algorithms that perform both power allocation and scheduling at the same time. That is, we are looking for the combination of users and power levels that optimize the performance of the network. This concept was briefly introduced when describing Round Robin scheduling in Subsection 3.3.1, and will be further explained and extended to multi-cell networks.

3.4.1 Maximum Capacity Scheduling

The Max-Cap algorithm is presented in [24], and is an extension to the single-cell Max-SNR scheduling. That is, taking interference and power control into account, we have a two step multi-cell scheduling algorithm.

First, for all user combinations $\mathbf{I}$ the power allocation $\mathbf{P}(\mathbf{I})$ and the corresponding achievable throughput $R(\mathbf{I}, \mathbf{P}(\mathbf{I}))$ is stored. Then, the users $\mathbf{I}^*$ that have the highest maximum sum throughput are scheduled. That is, we find tuples of users from each cell that maximizes capacity, and we transmit with the corresponding power levels given by $\mathbf{P}^*$.

Mathematically the algorithm can be expressed as follows:

$$(\mathbf{I}^*, \mathbf{P}^*) = \underset{\substack{\mathbf{I}\in\Psi \\ \mathbf{P}\in\Delta\Omega}}{\operatorname{argmax}} R\,, \tag{3.14}$$

where R is the system throughput, as defined in (3.7), $\mathbf{I}$ is the scheduled user vector, and $\mathbf{P}$ is the power allocation vector.

As mentioned in [24], the system capacity is maximized at the expense of fairness, but if all users have the same expected SNR and propagation channel, we will over a long enough time window still maintain fairness. In addition, the process of finding the optimal user and power selection is complex, thus Max-Cap scheduling is more interesting as a benchmark for possible performance than being implementable in practical systems.

3.4.2 Vectorized Proportional Fair Scheduling

The Vectorized Proportional Fair Scheduling (V-PFS) is this report's addition to the multitude of possible scheduling algorithms. The main idea behind V-PFS is to use the principles of Max-Cap scheduling, but replacing the metric with that of the PFS algorithm. This means that we have extended the PFS from single-cell to multi-cell networks and included power allocation in the optimization. Previously, PFS has been extended for multi-user [5] and multi-carrier [8] transmission systems.

Generally speaking, the expression for the vectorized proportional fair scheduling

algorithm is as follows:

$$(\mathbf{I}^*(t), \mathbf{P}^*(t)) = \underset{\substack{\mathbf{I}\in\Psi \\ \mathbf{P}\in\Omega}}{\operatorname{argmax}} \sum_{k=1}^{N} \left(\frac{R_{k|\mathbf{I}}(t)}{T_k(t)} \right) \tag{3.15}$$

$$T_k(t+1) = \begin{cases} (1-\frac{1}{i_c})T_k(t) + \frac{1}{i_c}R_{k|\mathbf{I}}(t), & k \in \mathbf{I}^*(t) \\ (1-\frac{1}{i_c})T_k(t), & k \notin \mathbf{I}^*(t) \end{cases}, \tag{3.16}$$

where $R_{k|\mathbf{I}}(t)$ is the rate for user $k \in \mathbf{I}$ at instant t, $T_k(t)$ is the average throughput for user k at instant t, and i_c is the time window. The variables are the same as for traditional PFS, but we now consider a vector, or tuple, of users since it is a scheduling for multi-cell networks. We also observe the addition of power allocation to the expression, making it a joint process as mentioned above.

The aim of V-PFS is to jointly schedule users and allocate power in a multi-cell environment. Thus, we achieve the combination of multiuser diversity with the fairness inherent in PFS. The proposed algorithm finds the optimal scheduling and power allocation by searching through all users in all cells for all power allocations. That is, we want to find a tuple of users which make a good match together, and consequently optimizes the metric for the algorithm. Since the rate of the users is a function of the SNIR, the power allocation and user selection must be done at the same time in order to find an optimal solution.

The following proposition gives an expression for multi-cell proportional fair scheduling as presented in [5].

Proposition 3. *Multi-cell proportional fair scheduling is expressed by:*

$$\mathbf{I}^*(t) = \underset{\mathbf{I}\in\Psi}{\operatorname{argmax}} \prod_{k=1}^{N} \left(1 + \frac{R_{k|\mathbf{I}}(t)}{(i_c-1)T_k(t)} \right). \tag{3.17}$$

Proof. We will show that equation (3.17) fulfills the criterium for a proportional fair scheduler. It is has been shown that a proportional fair scheduling algorithm should maximize:

$$\sum_k \log T_k(t). \tag{3.18}$$

We consider the following system objective function [5]:

$$\begin{aligned} J &= \sum_k \log T_k(t+1) \\ &= \sum_{k\notin\mathbf{I}} \log\left(\left(1-\frac{1}{i_c}\right) T_k(t) \right) + \sum_{k\in\mathbf{I}} \log\left(\left(1-\frac{1}{i_c}\right) T_k(t) + \frac{1}{i_c} R_{k|\mathbf{I}}(t) \right) \\ &= \sum_k \log\left(\left(1-\frac{1}{i_c}\right) T_k(t) \right) + \sum_{k\in\mathbf{I}} \log\left(1 + \frac{R_{k|\mathbf{I}}(t)}{(i_c-1)T_k(t)} \right). \end{aligned} \tag{3.19}$$

The first term in (3.19) can be omitted since it does not depend on the scheduling vector. Hence, we want to solve the following optimization problem:

$$\begin{aligned}\mathbf{I}^*(t) &= \underset{\mathbf{I}\in\Psi}{\operatorname{argmax}}\, J = \underset{\mathbf{I}\in\Psi}{\operatorname{argmax}} \sum_{k=1}^{N} \log\left(1+\frac{R_{k|\mathbf{I}}(t)}{(i_c-1)T_k(t)}\right) \\ &= \underset{\mathbf{I}\in\Psi}{\operatorname{argmax}} \log \prod_{k=1}^{N}\left(1+\frac{R_{k|\mathbf{I}}(t)}{(i_c-1)T_k(t)}\right). \end{aligned} \tag{3.20}$$

Applying that the logarithmic function is a monotonously increasing function, we can discard it, and we observe that (3.20) is equivalent with our original statement. □

As pointed out in [5], we can simplify (3.17) by investigating the following expression:

$$\begin{aligned}\mathbf{I}^*(t) &= \underset{\mathbf{I}\in\Psi}{\operatorname{argmax}} \prod_{k=1}^{N}\left(1+\frac{R_{k|\mathbf{I}}(t)}{(i_c-1)T_k(t)}\right) \\ &= \underset{\mathbf{I}\in\Psi}{\operatorname{argmax}} \left(1+\frac{R_{1|\mathbf{I}}(t)}{(i_c-1)T_1(t)}\right)\cdots\left(1+\frac{R_{N|\mathbf{I}}(t)}{(i_c-1)T_N(t)}\right) \\ &= \underset{\mathbf{I}\in\Psi}{\operatorname{argmax}} \left(1+\sum_{k=1}^{N}\frac{R_{k|\mathbf{I}}(t)}{(i_c-1)T_k(t)} + B\left(R_{1|\mathbf{I}}(t),\ldots,R_{N|\mathbf{I}}(t)\right)\right), \end{aligned} \tag{3.21}$$

where $B\left(R_{1|\mathbf{I}}(t),\ldots,R_{N|\mathbf{I}}(t)\right)$ is the by-products from the multiplication. If we consider that the user rates are independent, we can omit the by-products resulting in the following expression for multi-cell proportional fair scheduling:

$$\mathbf{I}^*(t) = \underset{\mathbf{I}\in\Psi}{\operatorname{argmax}} \sum_{k=1}^{N}\left(\frac{R_{k|\mathbf{I}}(t)}{T_k(t)}\right). \tag{3.22}$$

The expression has the same form as single-cell proportional fair scheduling, as we observe for the case where one cell is considered, where (3.22) leads to the same expression as for (3.11).

The proposition that follows combine multi-cell proportional fair scheduling and power control in a joint process, while still being proportional fair.

Proposition 4. *Joint multi-cell power allocation and proportional fair scheduling is proportional fair.*

Proof. We extend Proposition 3 to include power control, and we will show that the obtained expression is proportional fair.

When looking for the optimal solution, we search through all possible power levels as well as all scheduling vectors to see which combination maximizes the following expression:

$$\prod_{k=1}^{N}\left(1+\frac{R_{k|\mathbf{I}}(t)}{(i_c-1)T_k(t)}\right), \tag{3.23}$$

which is an extension of (3.17) as power control is included in the expression. Hence, we want to solve the following optimization problem

$$(\mathbf{I}^*(t), \mathbf{P}^*(t)) = \underset{\substack{\mathbf{I}\in\Psi \\ \mathbf{P}\in\Omega}}{\operatorname{argmax}} \prod_{k=1}^{N} \left(1 + \frac{R_{k|\mathbf{I}}(t)}{(i_c - 1)T_k(t)}\right). \tag{3.24}$$

The effect of the transmit power level is captured by the rate, and following the argumentation from Subsection 3.2.2, we see that performance can improve with power allocation. If we consider the explanation in Proposition 3 as emitting with full power in all cells being the worst-case scenario, the achievable throughput will improve by applying power control.

Since the expression for proportional fair scheduling is preserved, and the rate and average throughput take into account the selected power level, we can conclude that the joint power allocation and scheduling algorithm for multi-cell networks based on proportional fairness is indeed proportional fair. □

We have developed an expression for multi-cell power allocation and scheduling based on proportional fairness. The obtained results will be used in the following proposition to show how V-PFS is derived from (3.24), and to analyze the performance of the proposed joint power allocation and scheduling algorithm.

Proposition 5. *The proposed vectorized proportional fair scheduling algorithm is approximately proportional fair.*

Proof. The transformation of (3.20) to (3.22) is not valid with the introduction of power control, since the rates are no longer independent. Therefore we consider the following approximation:

$$\sum_{k=1}^{N} \log\left(1 + \frac{R_{k|\mathbf{I}}(t)}{(i_c - 1)T_k(t)}\right) \simeq \sum_{k=1}^{N} \frac{R_{k|\mathbf{I}}(t)}{(i_c - 1)T_k(t)}, \tag{3.25}$$

which is based on that $\log(1 + x) \simeq x$ for small values of x. We let $x = \frac{R_{k|\mathbf{I}}(t)}{(i_c-1)T_k(t)}$, and assume that the ratio rate-average throughput is close to unity, since the expected rate and the average throughput are of the same order of magnitude. Based on this assumption, x is a variable which depends on the ratio of a value close to unity and i_c. Since i_c is generally a large number, we can conclude that the approximation $\log(1+x) \simeq x$ is valid for a sufficiently large i_c.

We note that each term in the sum in (3.25) is approximated by $\log(1 + x) \simeq x$, which limites its validity to a moderate number of users. That is, with an increase in the number of users the total approximation error increases as well, since it is the sum of the approximation error in each term

Finding the power allocation and user scheduling that maximizes (3.25) is found by considering (3.20) and using the mentioned approximation, i.e., find

$$\begin{aligned}(\mathbf{I}^*(t), \mathbf{P}^*(t)) &= \underset{\substack{\mathbf{I}\in\Psi \\ \mathbf{P}\in\Omega}}{\operatorname{argmax}} \log \prod_{k=1}^{N} \left(1 + \frac{R_{k|\mathbf{I}}(t)}{(i_c-1)T_k(t)}\right) \\ &= \underset{\substack{\mathbf{I}\in\Psi \\ \mathbf{P}\in\Omega}}{\operatorname{argmax}} \sum_{k=1}^{N} \log \left(1 + \frac{R_{k|\mathbf{I}}(t)}{(i_c-1)T_k(t)}\right) \\ &\simeq \underset{\substack{\mathbf{I}\in\Psi \\ \mathbf{P}\in\Omega}}{\operatorname{argmax}} \sum_{k=1}^{N} \left(\frac{R_{k|\mathbf{I}}(t)}{(i_c-1)T_k(t)}\right), \end{aligned} \tag{3.26}$$

which is equivalent with (3.15), since $(i_c - 1)$ is a constant that we can discard when solving the optimization problem. Thus, vectorized proportional fair scheduling can be considered an approximation to joint multi-cell power allocation and proportional fair scheduling. □

The proof above shows that V-PFS compromises optimality in order to have a simpler expression for the optimization problem. In other words, we have an algorithm that is not strictly optimal, but as results in Section 5.3 show, the performance is close to optimal.

We note that for (3.15), the continuous domain of power allocation vectors is considered. Based on the recent advances in binary power control, we limit the domain to binary in this report, and benefit from its simplicity and low complexity, even though it is not strictly optimal for networks with more than two cells [25].

Performing an exhaustive search, V-PFS has worst-case complexity given by $\mathcal{O}(U^N 2^N)$, where U is the number of users in each cell, N the number of cells, and 2 comes from the fact that binary power allocation has two different power levels. The expression for the complexity follows by the fact that all combinations of users have to be checked for all power allocation combinations in order to find the tuple of users and the corresponding power levels that maximizes (3.15).

We note that V-PFS has a high complexity, but for small to moderate values of N, (3.15) is still easily computed. This makes the algorithm interesting as a benchmark for performance, and to give insight into how system capacity changes as a function of fairness.

Based on observations of proportional fair scheduling in different domains, we can present the following proposition.

Proposition 6. *Proportional fair scheduling for multi-carrier, multi-user and multi-cell transmission systems are equivalent.*

Proof. Analyzing the results from [5, 8] and Proposition 3, we see that all three are based on

$$\mathbf{I}^*(t) = \underset{\mathbf{I}\in\Psi}{\operatorname{argmax}} \prod_{k\in\mathbf{I}} \left(1 + \frac{R_k(t)}{(i_c-1)T_k(t)}\right), \tag{3.27}$$

where we assume that one user is only assigned one resource slot at a given moment.

The equality between the scheduling algorithms can be explained by observing that different domains are considered for all three, but the idea of a centralized proportional fair distribution lies behind for all. This can be illustrated by the following example:

1. Consider a two-carrier network with a group of users U.
2. Split the users in two groups, U_1 and U_2.
3. Assign U_1 and U_2 to frequency 1 and 2, respectively.
4. Move users in U_2 to a new cell denoted cell 2, while keeping users in U_1 in the original cell.
5. Assign users in cell 2 to the same frequency as cell 1, which completes the transformation from multi-carrier to multi-cell scheduling. □

To conclude this chapter on power allocation and scheduling, we present Table 3.2 which gives a resume of the subsections on the different scheduling algorithms.

Strategy	*Type*	*Characteristic*
Round Robin	Scheduling only	Ressource fair
Maximum SNR	Scheduling only	SNR maximizing
Proportional Fair	Scheduling only	Time window dependent
Maximum Capacity	Joint scheduling and power allocation	Capacity maximizing
Vectorized PFS	Joint scheduling and power allocation	Time window dependent

Table 3.2: Scheduling algorithm overview.

Chapter 4

Implementation

4.1 Overall structure

The simulations in this report is based on the numerical computing environment Matlab by Mathworks, and a simulation framework for wireless communications developed by PhD student Anders Gjendemsjø [6]. The structure of the software simulator is shown in Figure 4.1.

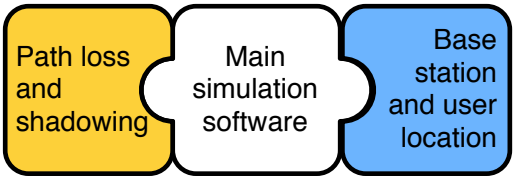

Figure 4.1: Overall program structure

The simulator structure is rather simple with its tripartition consisting of a main program, a channel manager, and a position manager. The main simulation software takes care of the power allocation and scheduling for the Monte Carlo iterations, while the channel manager calculates the values of path loss and shadowing for the channel gain matrix, and the position manager calculates the base station and user locations. The idea behind this separation is that we have a modularized system where the path loss model, shadowing or number of cells can be changed without affecting the main simulation program.

The described framework has been modified in order to implement the different power allocation strategies and the scheduling algorithms needed for the simulations in this report, without changing the overall composition of the wireless communications simulator. Even though the program structure is easy to understand, a considerable amount of time has been dedicated to understanding the background theory for the program and the effects of changing the parameters and algorithms on the obtained

simulation results. It has to be emphasized that the simple program structure is in contrast to the complexity of the optimization problem at hand.

4.2 Simulation model

The main objective of the simulations has been to investigate the fairness in full spectrum reuse hexagonal multi-cell networks. The simulations have focused on centralized algorithms for power allocation and scheduling, which requires a unit to process the CSI sent from the different cells and users before making a decision.

For all simulations, binary power allocation is applied, as it has proven its optimality for two-cell networks, and its close to optimal behaviour for multi-cell networks. This is done since we know from [25] how binary power control compares to the optimal power allocation found with the mathematical framework of geometric programming (GP)[1]. Hence, we have used binary power control (BPC) as the benchmark for the simulation, even though it is not proven to be strictly optimal for all scenarios.

We consider the following simulation scenarios for our hexagonal simulation setup. First, we will investigate the effect of increasing $P_{\min}$ in multi-cell networks. This is done by simulating a two-cell network with scheduling based on a variable number of users in each cell, followed by a multi-cell network with variable number of cells, but a fixed number of users. The goal is to see how BPC performs in terms of system capacity, when cells no longer can be completely turned off compared to not having adaptive power control.

Next, we consider different scheduling algorithms in two-cell networks, where we will simulate the RR, Max-Cap and V-PFS scheduling algorithms. This is to test the proposed V-PFS algorithm, and compare it to known scheduling algorithms to gain knowledge about its power consumption, system capacity and user selection. We will also test how the scheduling algorithms perform when $P_{\min}$ is increased.

Table 4.1 gives an overview over the system parameters used for the simulations, and we note that the scenarios differ in their values of $P_{\min}$ and the cell radius r.

The system is noise and interference impaired, and we model the received noise power as follows:

$$\sigma_i^2 = \sigma^2 = kTB, \tag{4.1}$$

where k is Boltzmann's constant, T the ambient temperature, and B the equivalent bandwidth. The parameters are defined as follows:

$$\begin{aligned} k &= 1.3806 \cdot 10^{-23}\ \mathrm{J/K} \\ T &= 290\ \mathrm{K} \\ B &= 1 \cdot 10^{6}\ \mathrm{MHz} \end{aligned}$$

We note that the additive noise is for simplicity modeled identically for all cells. The interference from neighbouring cells is defined by path loss, shadowing and multipath fading models, and is defined in the following section.

[1] For information about geometric programming including a tutorial, see [10].

System parameter	*Scenario a*	*Scenario b*	*Scenario c*	*Scenario d*
Carrier frequency	1800 MHz	1800 MHz	1800 MHz	1800 MHz
Cell radius r	1000 m	1000 m	5000 m	5000 m
Exclude disc radius	20 m	20 m	20 m	20 m
Base station height	30 m	30 m	30 m	30 m
Terminal height	1 m	1 m	1 m	1 m
Minimum transmit power	0 W	0.1 W	0 W	0.1 W
Maximum transmit power	1 W	1 W	1 W	1 W
Transceiver antenna gain	16 dB	16 dB	16 dB	16 dB
Receiver antenna gain	6 dB	6 dB	6 dB	6 dB
Shadowing standard deviation	10 dB	10 dB	10 dB	10 dB

Table 4.1: Simulation parameters

4.3 Path loss, shadowing and multipath fading models

The size of the hexagonal cells considered in this report dictates that the COST Walfisch-Ikegami model is the most appropriate path loss model. For larger macro-cells, the COST extension to the Hata model could be considered, but for the sake of simplicity, we stick to COST-WI path loss since it is also the one that fits best our simulation parameters. We note that it is the WI-LOS edition that is chosen.

The log-normal shadowing is modeled as a zero-mean gaussian variable with standard deviation 10 dB, which is within the range of 4 dB to 13 dB mentioned in [7]. Using a zero-mean Gaussian model for the distribution is justified when considering that there are many objects between the transmitter and the receiver, thus approximating the attenuation under the assumption that the shadowing is valid when applying the central limit theorem [7].

The COST-WI LOS model is an established model for cellular communications, and the choice of not implementing multipath fading has pros and cons, including a drop in system accuracy and reduced simulation complexity, respectively. However, the most important for our simulations is not the exact numerical results, but the trends we can observe when comparing different power allocation and scheduling algorithms. Thus, by selecting an appropriate model for the simulations as explained above preserving the important trends, we will get valid results.

4.4 Cell structure and layout

For the simulations considered in this report, we have used hexagonal cells, but it has to be underlined that the shape of cells is not important. That is, the analysis is valid for any geometry [24] even though only hexagonal cells are simulated.

Figure 4.2a presents a possible cell layout based on a hexagonal setup with 7 cells. To clarify, we have a center cell encircled by 6 other cells. The pattern, or cluster, presented in Figure 4.2a is repeated around a group of cells in the middle in Figure 4.2b as an

example of how small networks of cells can be used to model large cellular networks. This form of modelling is used in the cell wrap-around technique, which is a technique to simulated an infinite network with a finite model, and is explained in further detail in [6].

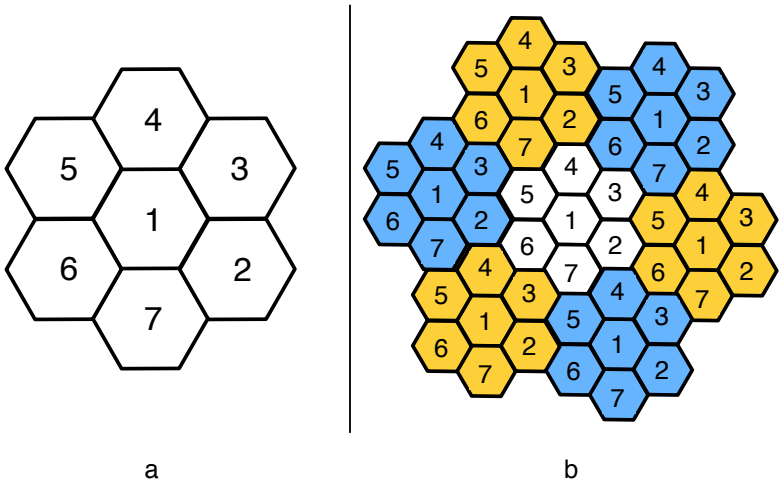

Figure 4.2: Hexagonal cell layout

We note that the number in each cell in Figure 4.2a illustrates the location of the cells in the simulations. That is, when using two-cell networks, cells 1 and 2 are used, and when using multi-cell networks with for instance 5 cells, cells 1 through 5 are used.

4.5 User distribution

The position manager deals with the distribution of users and their distance to the different base stations. To put another way, the users are spread out at random around their base stations, but not too close or too far from the BS. In order to get a uniform user distribution, we present the following procedure to draw users in a hexagon inscribed in a circle with radius r and center $(0, 0)$, as explained in [6].

1. Draw x and y uniformly from $[0, r]$ and $[-r, r]$, respectively.
2. Split each of the squares above and below the x-axis into two trapezoids according to
$$|y| + 3x > 2r \tag{4.2}$$
3. For all points (x, y) satisfying the condition above, they have to be flipped around and reassigned according to
$$\begin{aligned} x &:= x - r \\ y &:= \text{sign}(y)r - y \end{aligned} \tag{4.3}$$

4. Finally, the points (x, y) are scaled to fit the hexagon

$$x := \frac{3x}{2}$$
$$y := \frac{\sqrt{3}y}{2} \tag{4.4}$$

Figure 4.3 gives a graphic summary of the procedure of distributing the users, from the r by $2r$ square, to the r inscribed hexagon.

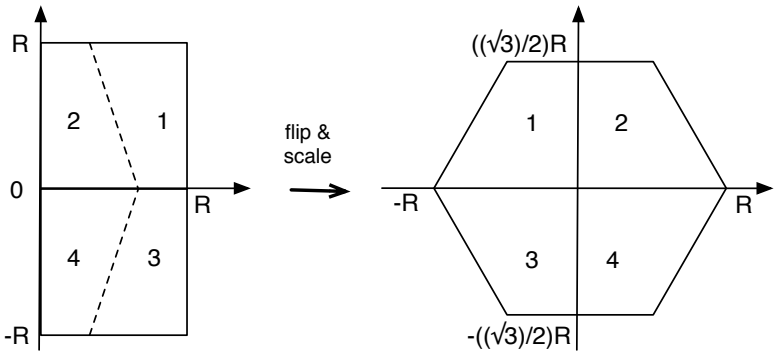

Figure 4.3: Generation of user locations

Some propagation models require a minimum distance between BS and UTs, which requires some additional attention. That is, for a minimum distance $d_{\min}$ the following condition has to be fulfilled

$$x^2 + y^2 > d_{\min}^2 \tag{4.5}$$

In other words, we create an exclusion disc around the base station with radius $d_{\min}$, and redraw the users that do not satisfy (4.5). In Matlab, this is done by adding a loop that checks the mentioned condition, which terminates once all users are in the desired area.

A possible user distribution with 7 users is illustrated by Figure 4.4, where the shaded x's are mobile user terminals, the antenna in the middle is the base station, and the circle at its base, the exclude disc radius.

The red shaded x is a user that falls on the inside of the exclude disc radius, and is consequently redrawn. The arrow shows the new position of the user, and the loop terminates since all users fulfill (4.5).

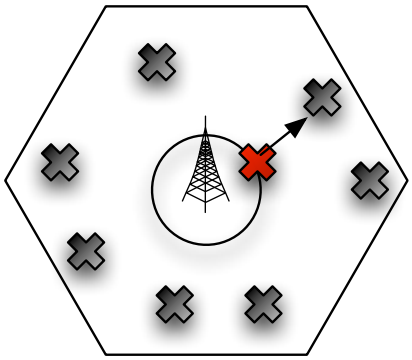

Figure 4.4: Sample user distribution in a hexagonal cell

Chapter 5

Simulation results

In this chapter we will present the results from simulations based on the different simulation scenarios explained in the previous chapter. The results are grouped into three sections; the first section investigates the effect of varying the level of $P_{\min}$ in both two-cell and multi-cell networks. The simulations for increased values of $P_{\min}$ are performed to observe the effect of introducing a notion of fairness on the average system capacity, since all users are guaranteed a minimum level of throughput when $P_{\min} > 0$.

The second section focuses on two-cell networks and the importance of scheduling algorithms with the goal of achieving an increase in capacity and a desired level of fairness simultaneously. That is, we consider scheduling as a method to smooth out any negative effects that binary power control might have on fair distribution of resources.

The third section investigates the loss in accuracy introduced by the approximation made for V-PFS. In other words, we compare the performance of V-PFS with that of M-PFS to see which impact the approximation has on system capacity and power consumption.

We defined four different simulation scenarios in Table 4.1 in order to observe the influence the system parameters have on the system capacity. The most important results are presented in this chapter, while additional simulation results for the simulation scenarios not presented here can be found in appendix A.

5.1 Binary power allocation with variable $P_{\min}$

5.1.1 Binary power control for two-cell case

The first simulation is based on a two-cell setup with hexagonal cells and a variable number of users in each cell. There is one user communicating with the BS at each time slot, selected with Max-Cap scheduling explained in Chapter 3.4.1.

First, we consider *scenario a* in Table 4.1, where Figure 5.1 illustrates two important observations concerning how the system capacity evolves as the number of users in each cell increases. First and foremost, the difference in system capacity between emitting with full power in both cells and using binary power allocation decreases as the number

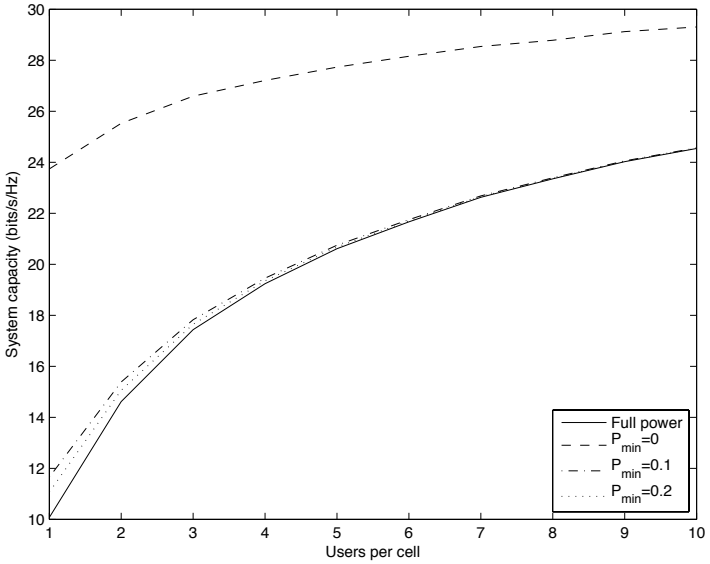

Figure 5.1: System capacity vs. users per cell for $r = 1000$ m and variable $P_{\min}$

of users in each cell increases. This is due to the fact that more users in a cell increase the possibility to select a user with good channel conditions, and consequently, having good users the system can transmit at maximum power more often.

Furthermore, the gain in capacity obtained using binary power allocation decreases drastically as the level of $P_{\min}$ increases. This phenomenon can be explained by considering on/off power allocation as a way to completely turn off interfering cells. When $P_{\min} > 0$, the system can no longer turn off interfering cells and the achievable gain rapidly decreases, since there will always be interference from neighbouring cells. Interestingly, we observe a significant drop in the capacity gain when we go from $P_{\min} = 0$ to $P_{\min} = 0.1$.

Hence, binary power allocation capacity converges to the capacity of transmitting with full power in all time slots as the number of users increases, and this convergence speeds up with increasing $P_{\min}$.

Table 5.1 summarizes the decrease in system capacity for four different power levels of $P_{\min}$ for a cell radius of $r = 1000$m. As mentioned, the most significant capacity drop occurs between when $P_{\min}$ no longer is 0, and both cells are on for all time slots. Since both cells are turned on, we could say that increasing $P_{\min}$ results in a loss of system capacity gain, but an increase in system fairness. This is because the system no longer turns off cells, and all cells can potentially transmit some data between a selected user and the base station.

By increasing the cell radius to $r = 5000$ m, which equals the parameters for *scenario b* from Table 4.1, we observe in Figure 5.2 that the throughput gain introduced by BPC has decreased. This can be explained by a greater distance to neighbouring cells, which

# Users	*P_{min}-level*	*System capacity*	*Loss*	*Normalized loss*
1	$P_{\min} = 0$	23.74	–	–
	$P_{\min} = 0.1$	11.66	50.89 %	88.43 %
	$P_{\min} = 0.2$	11.07	53.37 %	92.75 %
	$P_{\min} = P_{\max}$	10.08	57.54 %	100 %
5	$P_{\min} = 0$	27.74	–	–
	$P_{\min} = 0.1$	20.74	25.23 %	98.18 %
	$P_{\min} = 0.2$	20.68	25.45 %	99.02 %
	$P_{\min} = P_{\max}$	20.61	25.70 %	100 %

Table 5.1: System capacity for different values of $P_{\min}$ for $r = 1000$ m

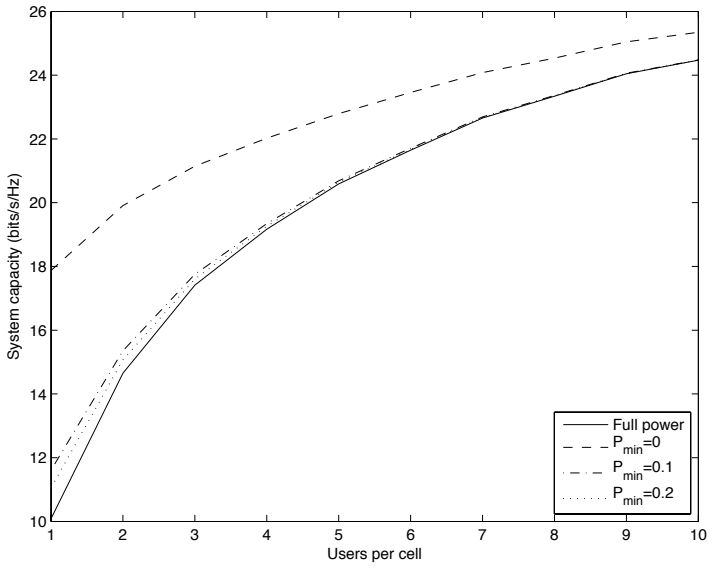

Figure 5.2: System capacity vs. users per cell for $r = 5000$ m and variable $P_{\min}$

means that the level of inter-cell interference is lower. That is, the gain of turning off cells has decreased, and more cells are turned on when the cell radius is greater. Accordingly, an increase in $P_{\min}$ does not affect the system capacity as much as for smaller cells.

# Users	P_{min}*-level*	*System capacity*	*Loss*	*Normalized loss*
1	$P_{\min} = 0$	17.87	–	–
	$P_{\min} = 0.1$	11.61	35.03 %	80.44 %
	$P_{\min} = 0.2$	11.06	38.11 %	87.59 %
	$P_{\min} = P_{\max}$	10.09	43.54 %	100 %
5	$P_{\min} = 0$	22.79	–	–
	$P_{\min} = 0.1$	20.69	9.24 %	95.65 %
	$P_{\min} = 0.2$	20.64	9.45 %	97.79 %
	$P_{\min} = P_{\max}$	9.66	25.70 %	100 %

Table 5.2: System capacity for different values of $P_{\min}$ for $r = 5000$ m

Nevertheless, Figures 5.1 and 5.2, and Table 5.1 show that other measures than increasing $P_{\min}$ have to be considered if we want to keep the gain achieved with binary power allocation and still improve the system fairness.

5.1.2 High and low SNIR simulations for two-cell case

Based on the results in the previous subsection, we decide to further investigate the effects of power level and noise on the system capacity for binary power allocation. We distinguish between two cases for the following simulations; high and low SNIR. The high SNIR scenario is the standard simulation environment, whereas the low SNIR scenario is introduced to observe the effect of a higher noise level.

The simulations are performed with very low minimum power levels to investigate the transition in system capacity when $P_{\min}$ is changed from 0 to being always on, i.e. $P_{\min} > 0$. We observe a loss in capacity gain due to the increase in the minimum transmit power level, as expected considering the results in Subsection 5.1.1.

Figure 5.3 presents the high SNIR scenario, and we observe the same trends as presented earlier. That is, an important drop in the capacity gain occurs when going from 0 to always having a minimum level of data transmission, which in this case is 0.0001. We note that the system capacity increases as $P_{\min} \to 0$, and the maximum capacity is achieved for $P_{\min} = 0$.

Interestingly, we observe a much smoother transition between $P_{\min} = 0$ and $P_{\min} = P_{\max}$ than in Figure 5.1, which is due to the very low power levels considered here.

In Figure 5.4 we have increased the level of the noise present in the network, and we observe a more compact figure. That is, the difference between the full power scheme and the binary power allocation is smaller. This can be explained by the fact that a greater noise level makes the interference less important, and the effect of turning off interferers is naturally weakened. Still, there is a loss in capacity gain associated with increasing the minimum transmit power level.

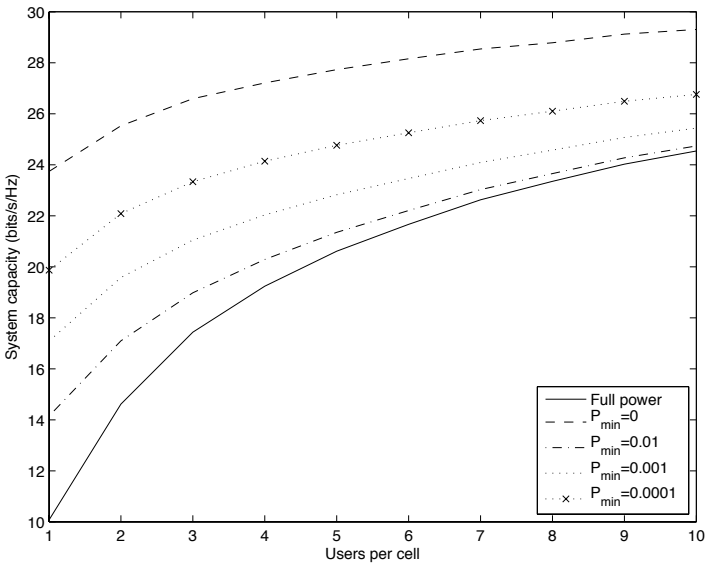

Figure 5.3: System capacity vs. users for high SNIR, $r = 1000$ m and variable $P_{\min}$

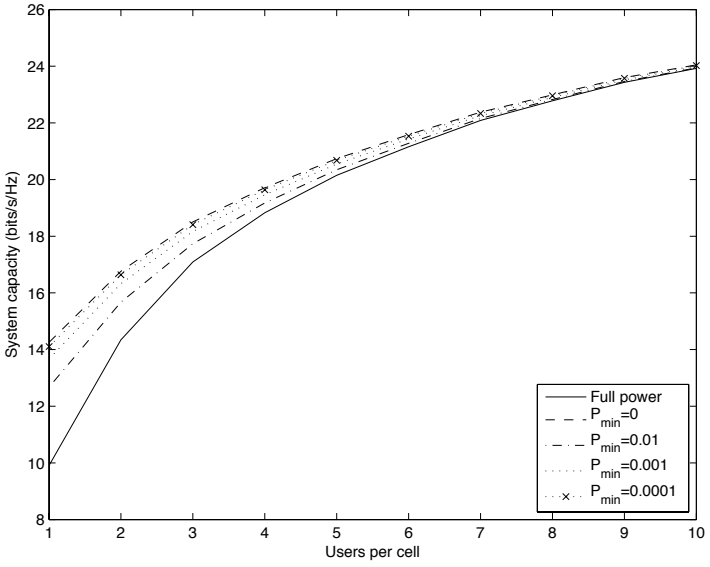

Figure 5.4: System capacity vs. users for low SNIR, $r = 1000$ m and variable $P_{\min}$

5.1.3 Binary power control for multi-cell case

This is an extension to the simulations in Subsection 5.1.1, which investigates the achievable capacity for binary power allocation with various $P_{\min}$ levels in a multi-cell environment with one user per cell. The reason for only having one user in each cell, is that the gain achieved by turning off interfering cells is largest when it is still possible to select users with poor channel conditions. In other words, with many users the probability of picking a user with good channel quality is high, fewer cells would be switched off, and consequently, the gain of turning off cells would be lower, making it more difficult to see the power allocation gain.

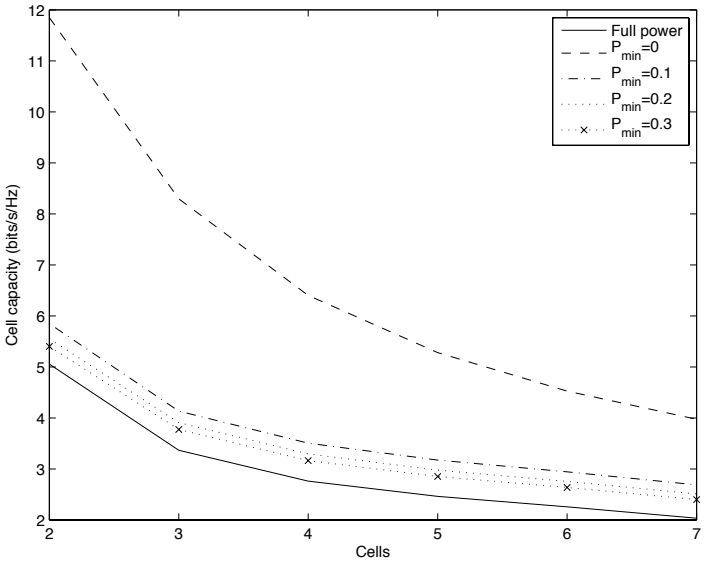

Figure 5.5: Cell capacity vs. cells for $r = 1000$ m and variable $P_{\min}$

Figure 5.5 shows a drop in the capacity per cell when the number of cells increase for all levels of $P_{\min}$, where the decrease in cell capacity seem to stabilize with the increasing number of cells. This decrease is understandable since the achievable per cell capacity is a function of the signal to noise-plus-interference ratio, which again depends on the number of interfering cells. In other words, the change of the interference level is higher when going from 2 to 3 cells, than when going from 5 to 6 cells, because the proportion of new interferers is lower.

We also observe that a significant drop in capacity occurs when we go from on/off power allocation to $P_{\min} = 0.1$, as already mentioned. That is to say that the differences between the consecutive increases in $P_{\min}$ are smaller. In other words, when the level of $P_{\min}$ no longer is zero, most of the gain achieved with the introduction of binary power allocation is lost, but with a gain in system fairness in some sense, since all users get a minimum throughput.

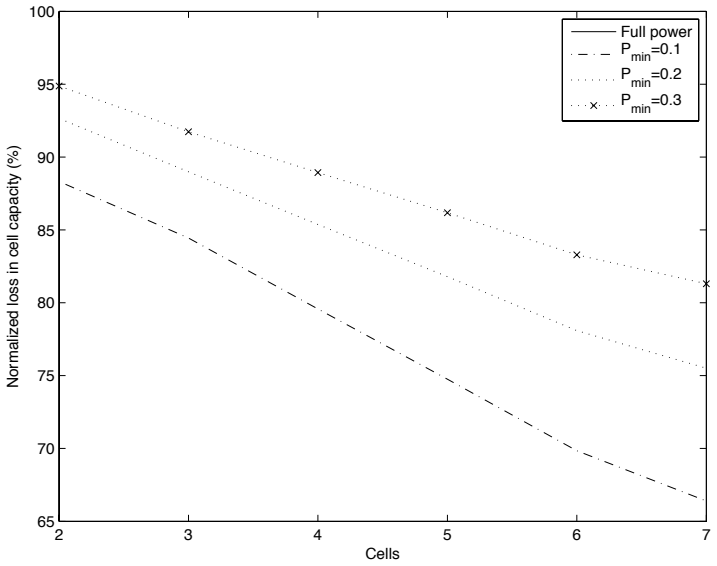

Figure 5.6: Normalized capacity loss vs. cells for $r = 1000$ m and variable $P_{\min}$

We observe that large parts of the gain achieved by the binary power allocation are lost with an increasing $P_{\min}$ in figure 5.6, which shows the normalized loss in capacity gain. That is, the loss introduced by using $P_{\min}$ larger than 0, where $P_{\min} = 0$ gives 0% loss and $P_{\min} = P_{\max}$ indicates 100% loss. It is interesting to note that going from $P_{\min} = 0$ to $P_{\min} = 0.1$ reduces the gain of the adaptive power scheme with over 60 %, in the best case.

When the number of cells increases, we observe that the drop in the normalized capacity loss decreases. This happens as the change in interference becomes less important as more cells are included in the simulations.

Figure 5.7 presents the average power consumption for the different $P_{\min}$ levels as a function of the number of cells, where we can see that the average power consumption is (slowly) decreasing. This can be explained by the fact that with more cells, the probability of turning off cells when the channels are bad is growing as the number of cells is increasing. In other words, with many cells there is a higher probability for the cells to be interfering with each other.

From Table 5.3 we observe that cells more often are turned off when $P_{\min} = 0$ than for $P_{\min} > 0$. In other terms, increasing $P_{\min}$ reduces the chance of having cells emitting with $P_{\min}$. Thus, the network will more often emit with $P_{\max}$ resulting in a higher power consumption and consequently more interference.

We also note the small difference in the values for $P_{\min} > 0$, which indicates that for the simulation values considered here, the most important change happens when we go from $P_{\min} = 0$ to $P_{\min} > 0$. As shown in the previous subsection, a more gradual change in the minimum transmit power level will give a less noticeable difference in system

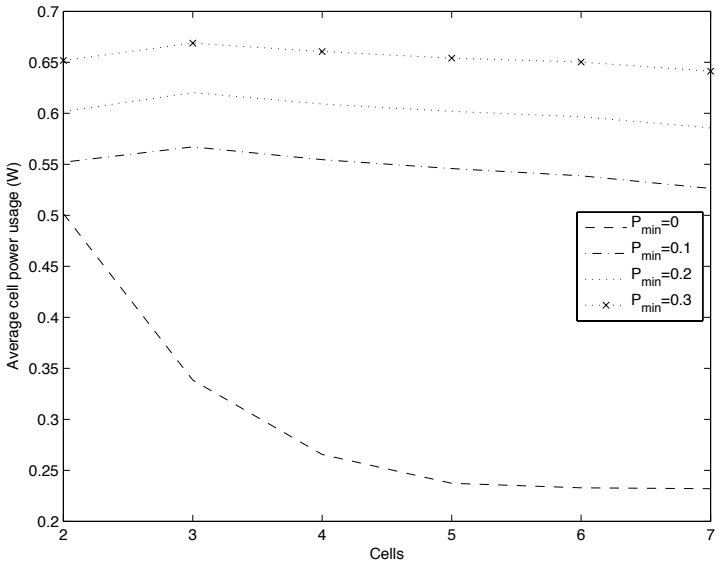

Figure 5.7: Average power vs. cells for $r = 1000$ m and variable $P_{\min}$

# Cells	$P_{min} = 0$	$P_{min} = 0.1$	$P_{min} = 0.2$	$P_{min} = 0.3$
2	50.17 %	50.22 %	50.24 %	50.26 %
3	33.85 %	51.90 %	52.53 %	52.69 %
4	26.56 %	50.51 %	51.14 %	51.51 %
5	23.73 %	49.54 %	50.24 %	50.59 %
6	23.28 %	48.74 %	49.59 %	50.04 %
7	23.20 %	47.37 %	48.22 %	48.76 %

Table 5.3: Percentage of cells emitting with $P_{\max}$ for $r = 1000$ m

capacity and power consumption.

The most important finding concerning both the two-cell and the multi-cell cases is that raising the level of $P_{\min}$ results in lower cell capacity and higher power consumption. In addition, the change from $P_{\min} = 0$ to $P_{\min} > 0$ gives a significant drop in cell capacity, because cells no longer can be completely turned off.

More simulation results, including the simulations for $r = 5000$m, i.e., *scenario c* and *scenario d*, can be found in Appendix A.1.1.

In the next section, the vectorized proportional fair scheduling algorithm, presented in Chapter 3.4.2, is simulated and compared with other scheduling algorithms to see whether it can improve fairness without compromising the gain achieved with binary power allocation.

5.2 Joint scheduling and power allocation performance

5.2.1 On/off power allocation

The objective for the following simulations is to highlight the performance for the RR, Max-Cap and V-PFS scheduling algorithms, which are explained in Sections 3.3 and 3.4. The parameters are the same as for the previous two-cell case as given in *scenario a* in Table 4.1.

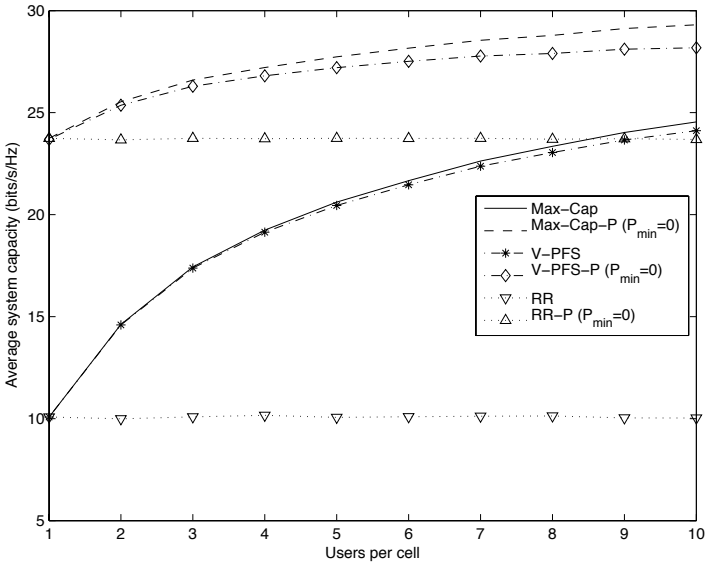

Figure 5.8: Average system capacity vs. users for $P_{\min} = 0$

Figure 5.8 shows the performance of the three different algorithms. It is noteworthy that they gather in two groups; one group for the algorithms that can adaptively choose to turn off cells, marked with a -P, and one group for the algorithms that emit with constant power, i.e., $P_{\min} = P_{\max}$.

The round robin (RR) algorithm has the poorest performance, where the system capacity remains constant as the number of users increases. This is due to the fact that users are selected independently of channel quality and are given an equal part of the available resources, making the obtained capacity over many simulations the average capacity a user can achieve. We observe that the algorithm does not take advantage of the variability in user channels. When the possibility to adapt the power levels in the two cells, denoted by RR-P, we observe an increase in performance due to the possibility to turn of interferers. Still, the system capacity remains constant as the number of users in each cell increase, as expected.

The maximum capacity (Max-Cap) algorithm has the best performance of the three algorithms, since it selects the pair of users that maximizes system capacity. The dif-

ference between the adaptive, Max-Cap-P, and the fixed power allocation, Max-Cap, versions decreases as the number of users increase. That is, the gain achieved from turning off interferers becomes smaller as the number of users increase, since the chance of picking a user with a good channel is higher. Consequently, the chance finding pairs of users is also higher, thus fewer cells are turned off.

The novel vectorized proportional fair scheduling (V-PFS) algorithm performs similarly to the Max-Cap algorithm; with adaptive power allocation, V-PFS-P, starts like RR-P and Max-Cap-P, but looses in capacity to the Max-Cap algorithm because V-PFS-P takes fairness into account. We observe the same behaviour for V-PFS and Max-Cap, that is, when we have no adaptation in the power allocation, they start with the same capacity, but V-PFS' increase slow down more. How close V-PFS performs to Max-Cap depends on the time horizon parameter i_c, as explained in Chapter 3.3.3, where the parameter is set to $i_c = 100$ in Figure 5.8.

The adaptive and the fixed power allocation versions end up having the similar performance when the number of users increases, since the possibility of choosing users with good channels increase as the number of users increase. Therefore, there is a higher probability for both cells being on, and eliminating the difference between the two capacity-wise. We note that RR is exempt from this characterization, since it does not benefit from the varying channel conditions in order to improve throughput.

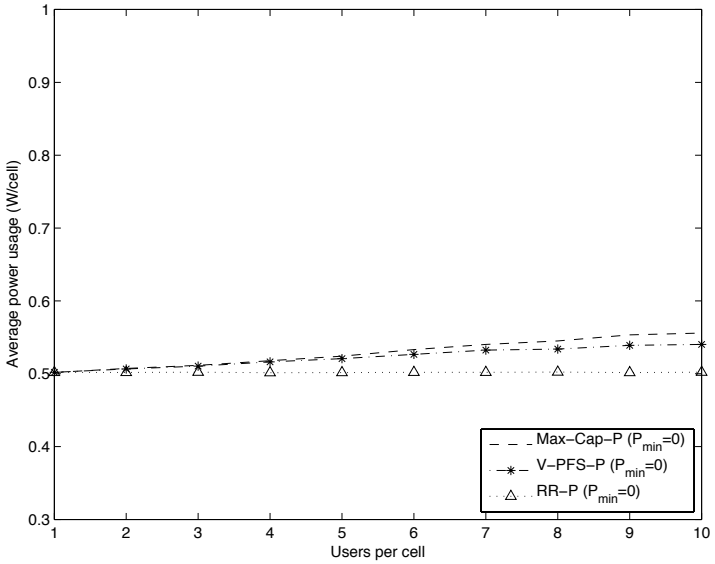

Figure 5.9: Average power usage vs. users for $r = 1000$ m and $P_{\min} = 0$

The power consumption for the different adaptive techniques is shown in Figure 5.9. RR-P, Max-Cap-P and V-PFS-P all start at the same point, but RR-P has a constant power consumption, whereas Max-Cap-P and V-PFS-P have an increasing power consumption as the number of users increase. This can be explained with the fact that the

Round Robin algorithm selects users on a turn by turn basis and has the same average capacity and power consumption independently of the number of users.

Max-Cap-P and V-PFS-P have similar power allocation strategies, with V-PFS-P having the lowest power consumption of the two. This is due to the fact that V-PFS-P has a higher percentage of solutions with one of the cells turned off than Max-Cap-P, which can be explained by the fact that V-PFS-P selects users and power allocation based on a fairness metric, and not necessarily which users that maximizes system capacity.

It is worth noting that RR has the lowest power consumption of all three considered algorithms, but, as observed in Figure 5.8, has significantly inferior system capacity with an increasing number of users in each cell, and is therefore not particularly interesting as strategy.

# Users	*Algorithm*	(P_{max}, P_{min})	(P_{min}, P_{max})	(P_{max}, P_{max})
1	RR-P	50.25 %	49.4 %	0.35 %
	Max-Cap-P	50.25 %	49.4 %	0.35 %
	V-PFS-P	49.81 %	49.81 %	0.38 %
4	RR-P	51.07 %	48.63 %	0.30 %
	Max-Cap-P	48.75 %	47.67 %	3.58 %
	V-PFS-P	48.28 %	48.44 %	3.28 %
7	RR-P	50.43 %	49.18 %	0.39 %
	Max-Cap-P	46.45 %	45.49 %	8.06 %
	V-PFS-P	46.72 %	46.80 %	6.48 %
10	RR-P	49.49 %	50.08 %	0.43 %
	Max-Cap-P	44.41 %	44.41 %	11.18 %
	V-PFS-P	46.00 %	45.96 %	8.04 %

Table 5.4: Power allocation overview for $r = 1000$ m, $i_c = 100$, and $P_{\min} = 0$

The power allocation overview in Table 5.4 shows that the Max-Cap-P and V-PFS-P algorithms have similar power allocation strategies, as already mentioned for Figure 5.9. The explanation for V-PFS-P's lower power consumption than Max-Cap-P is that one of the cells is more frequently turned off. We note that the power consumption shows that one cell is turned off almost all the time, which indicates that the level of interference is considerable for this simulation scenario.

In order to better understand the manner of operation of the scheduling algorithms in terms of throughput and user selection, we analyze the way users are chosen by the algorithms in Figure 5.10. Blue bars indicate the algorithms pick the same pair of users, green bars indicate that the algorithms differ in one of the users in the selected pair, and red bars indicate a completely different selection of user pairs.

The figure on top shows the comparison in user selection for Max-Cap-P and V-PFS-P. We observe that with only one user in each cell, the two algorithms obviously pick the same user. As the number of users increases, we observe that Max-Cap-P and V-PFS-P select the same users for the majority of time slots. At the same time, we note that the percentage of one or both users being different is steadily increasing as more users are

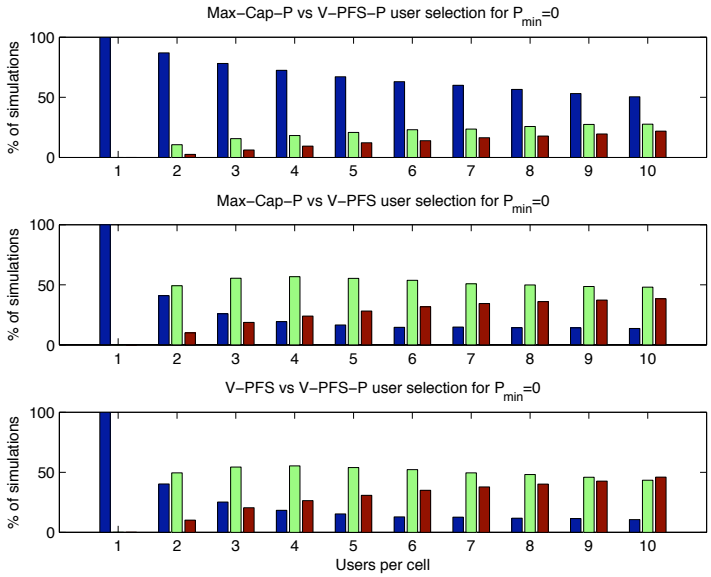

Figure 5.10: User selection comparison for Max-Cap-P, V-PFS and V-PFS-P

simulated in each cell.

In the middle, we observe that the way users are chosen for Max-Cap-P and V-PFS has some of the same characteristics as for Max-Cap-P and V-PFS-P. That is, both algorithms start by selecting the same users, but V-PFS more often selects one or both users differently. This is due to the fact that V-PFS is not able to adapt emitted power, and therefore different users are selected in order to obtain optimal rate-average throughput metric.

The lowermost figure illustrates the differences between V-PFS and V-PFS-P when it comes to the users the two versions of the V-PFS algorithm select. As suggested in the middle figure, V-PFS and V-PFS-P does not necessarily select the same user pair, which is confirmed in the lowermost figure. This is due to that they have different average rates for the different users, $T_k(t)$, and therefore the maximization of the metric can end up giving different users.

We note that the different system capacities presented in Figure 5.8 is explained by the results in Figure 5.10. To clarify, the reason for the different system capacites is that the scheduling algorithms select different users in order to maximize the metric associated with the algorithm. Hence, different user pairs result in different capacities.

For more simulation results for increased values of i_c and r, and for detailed plots on how the V-PFS, V-PFS-P and Max-Cap-P algorithms distribute users and rates, see Appendix A.2.1.

5.2.2 Binary power allocation with variable $P_{\min}$

These are the results for the simulations with $P_{\min} = 0.1$, but all other parameters remain the same as the previous case, which corresponds to *scenario b* in Table 4.1.

First and foremost, we observe the same trends as in previous simulations, where the most interesting result is that the average system capacity of the adaptive and non-adaptive algorithms become almost equal. We do also observe a rather significant drop in average system capacity in Figure 5.11 for all adaptive types of the three scheduling algorithms with the increase in $P_{\min}$.

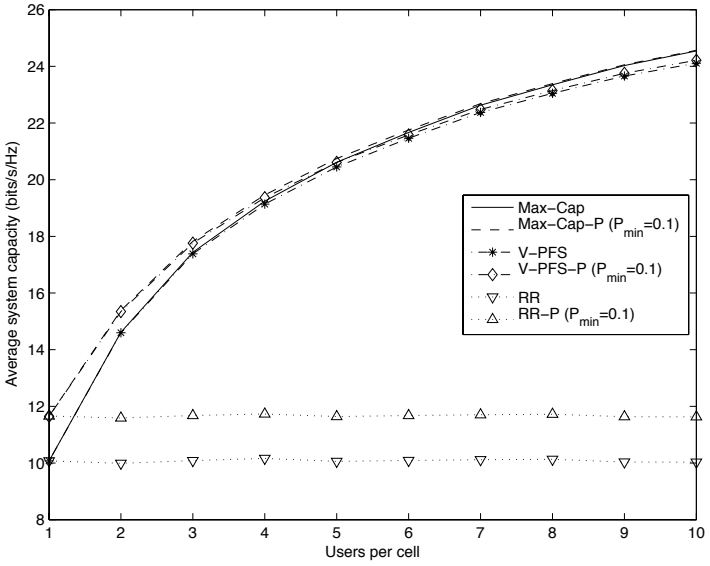

Figure 5.11: Average system capacity vs. users for $P_{\min} = 0.1$

In addition to these trends, we observe that RR-P and V-PFS-P have almost equal power consumption in Figure 5.12, while Max-Cap-P has a slightly higher average power usage. This observation is also visible in Table 5.5, where we see that with an increase in $P_{\min}$, the Max-Cap algorithm more often transmit with both cells.

Figure 5.13 illustrates the user selection for Max-Cap-P, V-PFS-P, and V-PFS, in the same way as for Figure 5.10. There is a remarkable change in the choice of users compared to the case when $P_{\min} = 0$ in Figure 5.10. The majority of the selected users are now the same, independently of algorithm. The way the users are selected can be explained by a higher level of interference from neighbouring cells, and scheduled users are more often the same, if not all the time, for $P_{\min} > 0$. In other words, higher power levels mean more interference, which means that ideal users are the same for all algorithms.

We note that the selected users for V-PFS-P and V-PFS are for the majority of time slots the same. In other words, the adaptive and static versions of the V-PFS

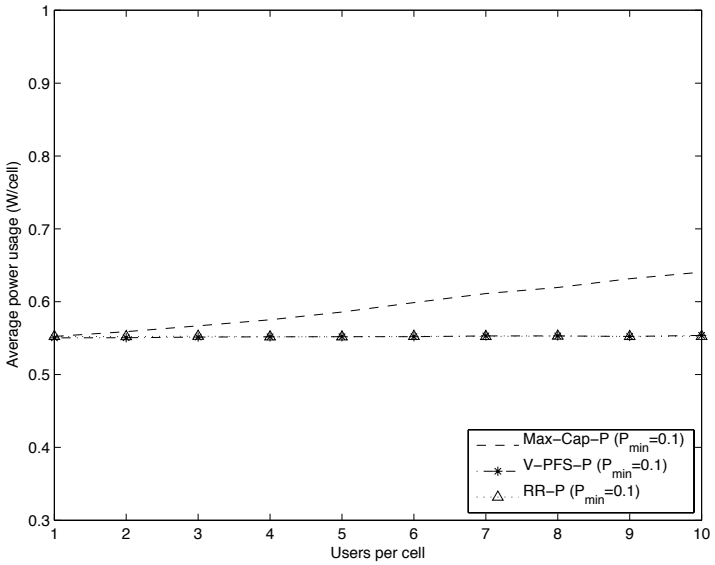

Figure 5.12: Average power usage vs. users for $P_{\min} = 0.1$

# Users	*Algorithm*	(P_{max}, P_{min})	(P_{min}, P_{max})	(P_{max}, P_{max})
1	RR-P	50.46 %	49.01 %	0.53 %
	Max-Cap-P	50.46 %	49.01 %	0.53 %
	V-PFS-P	49.76 %	50.17 %	0.07 %
4	RR-P	49.72 %	49.88 %	0.40 %
	Max-Cap-P	47.80 %	47.61 %	5.59 %
	V-PFS-P	49.5 %	50.1 %	0.40 %
7	RR-P	50.09 %	49.39 %	0.52 %
	Max-Cap-P	43.09 %	43.33 %	13.58 %
	V-PFS-P	49.67 %	49.66 %	0.67 %
10	RR-P	49.59 %	49.86 %	0.55 %
	Max-Cap-P	39.72 %	40.13 %	20.15 %
	V-PFS-P	49.63 %	49.53 %	0.84 %

Table 5.5: Power allocation overview for $r = 1000$ m, $i_c = 100$, and $P_{\min} = 0.1$

algorithm have an insignificant difference difference in user scheduling, which follows from the paragraph above.

In addition, the small difference in the way users are selected reflects over to the system capacity. As illustrated in Figure 5.11, the system capacity for the different algorithms have more similar characteristics than for $P_{\min} = 0$ in Figure 5.8. That is, the gain introduced by using binary power control is reduced, making the difference in system capacity between the adaptive and static power allocation decrease. In some sense, an increase in the minimum transmit power level is equivalent with a reduction in the freedom of choice for the optimization.

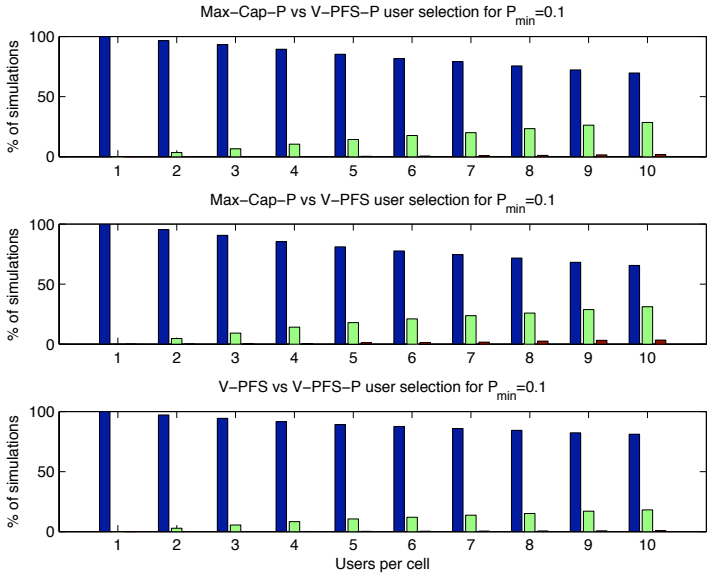

Figure 5.13: User selection comparison for Max-Cap-P, V-PFS and V-PFS-P

Additional simulation results for time horizon $i_c = 1000$, and $r = 5000$ m corresponding to *scenario c* and *scenario d* can be found in Appendix A.2.2.

5.3 Performance comparison for V-PFS

The mathematical derivations in Subsection 3.4.2 showed that V-PFS is not strictly optimal, since it is based on an approximation of the expression for joint multi-cell power allocation and proportional fair scheduling. We wanted to investigate the effect of this approximation on the performance for the proposed algorithm. The two following subsections describe the results found when comparing V-PFS with the an optimal algorithm for joint multi-cell power allocation and proportional fair scheduling, denoted as M-PFS.

5.3.1 On/off power allocation

This scenario is known as *scenario a* from Table 4.1, where the trends are the same as explained earlier. That is, algorithms with power control is found as the group with highest capacity, while the algorithms without power control comprise the group with lowest throughput. In addition, the Max-Cap algorithm outperforms the PFS based algorithms with its goal of maximizing capacity.

We observe in Figure 5.14 that M-PFS and V-PFS, and M-PFS-P and V-PFS-P have close to identical system capacity. Hence, the approximation made for V-PFS has little effect on its performance when it comes to throughput.

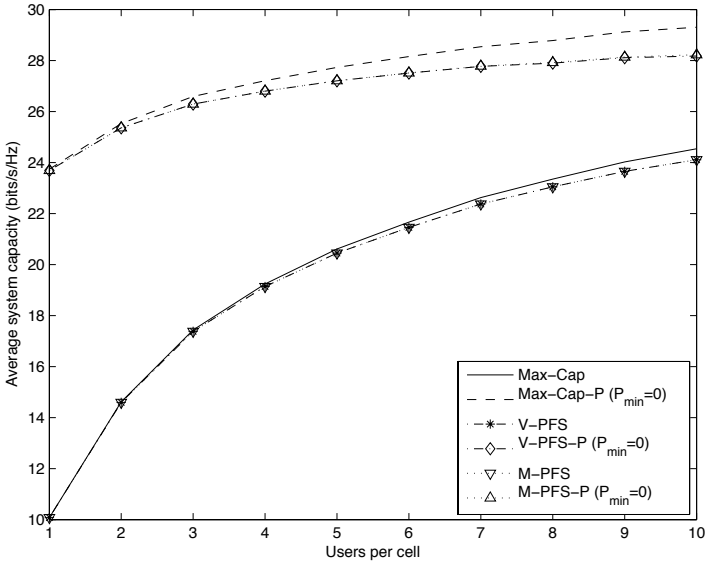

Figure 5.14: System capacity for PFS for $r = 1000$ m, $i_c = 100$ and $P_{\min} = 0$.

When comparing the power consumption, Figure 5.15 illustrates that M-PFS-P and V-PFS-P have different power allocations. To clarify, M-PFS and V-PFS have similar throughputs, but do not allocate power in the same manner. This is the result of the decoupling of the rates for the different cells, and more cells are turned off than strictly optimal.

5.3.2 Binary power allocation with variable $P_{\min}$

In this subsection we analyze the results when simulating with the parameters defined in *scenario b* from Table 4.1, in order to see the effects of the utilised approximation for binary power allocation with $P_{\min} = 0.1$.

Figure 5.16 shows the general result of increasing the minimum transmit power level. We also see that the M-PFS and V-PFS, and M-PFS-P and V-PFS-P are almost identical

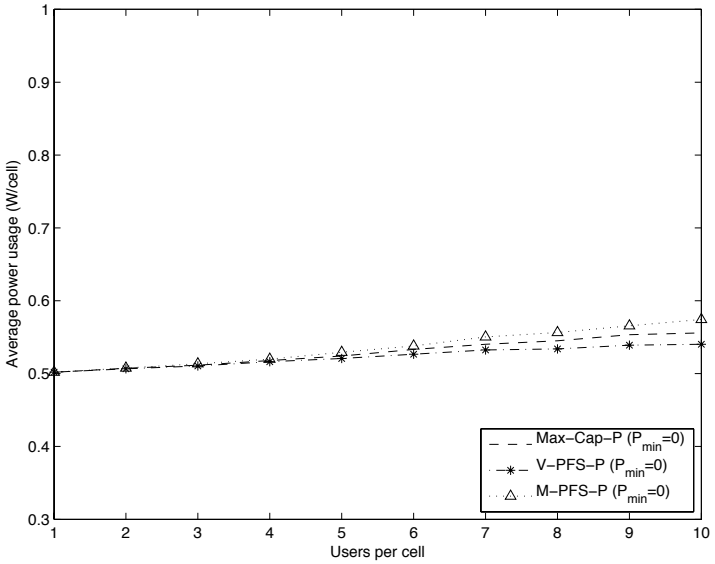

Figure 5.15: Power consumption for PFS for $r = 1000$ m, $i_c = 100$ and $P_{\min} = 0$.

performance-wise. This equality is twofold; firstly, we observe once again that there is a negligible difference in system capacity between M-PFS and V-PFS. Secondly, when increasing $P_{\min}$ the difference between the algorithms with and without power control decreases, i.e. PFS and PFS-P are equal when the number of users increase.

When considering the power consumption in Figure 5.17 for the two different algorithms, we observe the same trends as in Figure 5.15. That is, V-PFS-P has lower power consumption than M-PFS-P, and turns off more cells than the optimal solution.

Hence, the approximation used for V-PFS can be considered as valid, and V-PFS yields almost identical performance as an optimal joint multi-cell power allocation and proportional fair scheduling algorithm.

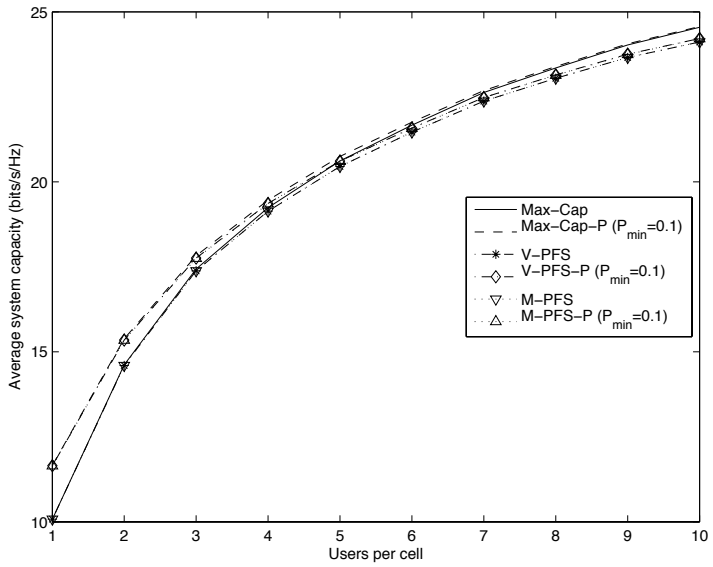

Figure 5.16: System capacity for PFS for $r = 1000$ m, $i_c = 100$ and $P_{\min} = 0.1$.

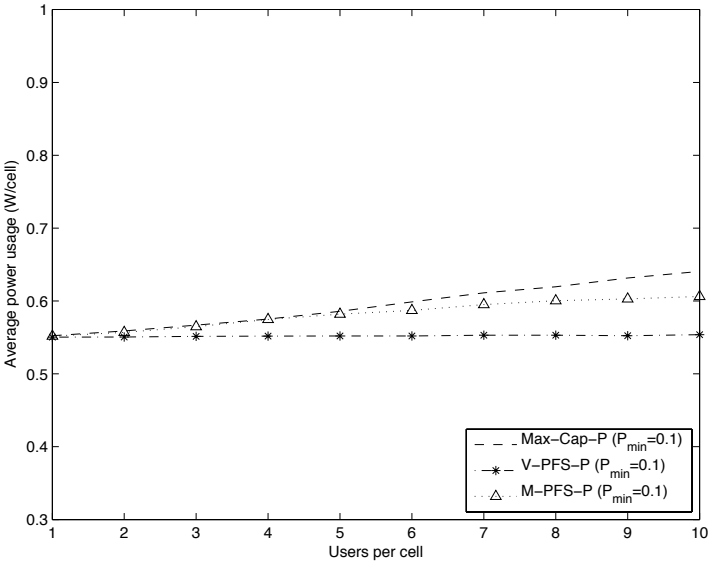

Figure 5.17: Power consumption for PFS for $r = 1000$ m, $i_c = 100$ and $P_{\min} = 0.1$.

Chapter 6

Discussion

6.1 System parameters

The simulations are based on assumptions and models for path loss, shadowing and multipath fading, where the latter was chosen not to be implemented, as a trade-off between result accuracy and simulation scope. That is, the precision of the results would be better with multipath fading, but they would also require a higher number of repetitions for the Monte Carlo simulations. In addition, with multipath fading, we would have an increase in system capacity since the fading introduces randomness to the channel and scheduling would let the system benefit from this randomness by applying the concept of riding the peaks [20].

Regarding the cell radius for the networks simulated in this report, two sizes have been tested to investigate the effect it has on the results. Observing more or less the same trends for both cases, it leads us to think that the used model is accurate and the results are valid. Nevertheless, for the small cell radius, the amount of cells turned off because of the high interference from neighbouring cells might be an indication that a LOS model is not appropriate for so small cells. That is, small cells could be considered representing a city environment where LOS would be difficult to achieve due to buildings, trees and other obstacles between the BS and the UTs.

The noise present in the system could be considered too small for the cell simulations with small radii. Or, the other way round, the transmitted power level could be considered too high when simulating small cells. At the same time, it demonstrates how parameters as cell size, power level and noise level all affect the achievable throughput.

6.2 The level of $P_{\mathbf{min}}$

Through the introduction of binary power control in multi-cell networks, we observe a gain in average system capacity compared to emitting with full power in all cells. This gain is obtained by having the possibility to turn off interferers. That is, cells that contribute more in interference than their raise in capacity are turned off, and we thereby achieve an increase in the overall system capacity.

When the minimum power level, $P_{\min}$, is raised, there is a significant drop in the gain in capacity achieved with binary power allocation. The importance of the loss in capacity gain depends on the chosen power level, where a level close to 0 gives a throughput close to that off on/off power allocation. The explanation for the capacity loss follows the same reasoning as above, but considering that cells cannot be completely shut down, there will always be a certain level of interference. Thus, there is still a gain compared to the full power scheme, but not as interesting as for the case $P_{\min} = 0$.

In some sense, an increase in $P_{\min}$ is equivalent to an increase in fairness, since all cells in the network may transmit with a minimum data rate all the time. That is, we have a system with high and low power levels, which corresponds to high and low data rates, and a minimum level of quality of service (QoS) is assured. Knowing that we need to transmit pilot signals and channel information, we have to have $P_{\min} > 0$.

There is again a conflict between maximizing capacity and maximizing fairness, which in this case is about how much loss in the BPC gain we are willing the sacrifice to let all cells have a minimum level of throughput at all times. When making the decision, it has to be considered that even a small increase in $P_{\min}$ drastically lowers system capacity.

6.3 Joint scheduling and binary power allocation

The majority of the simulations in this report concerns the combination of scheduling and binary power allocation. That is, we take advantage of the simplifications and the (sub)optimality of binary power control, when we perform the joint optimization of power and user scheduling. This is already a complex procedure with users, number of cells and power levels as degrees of liberty, and adding the process of scheduling users to this makes it even more complicated.

The performance of the V-PFS algorithm is as promised and expected, since it is based on PFS. That is, the average system capacity achieved with V-PFS can be arbitrarily close to that of Max-Cap, by adjusting the value for the time window, i_c, which decides the horizon for fairness. Thus, we have the opportunity to adapt the value of i_c in order to get the wanted capacity-fairness combination, depending on the system.

Evidently, this centralized way of controlling users and power is too complex to be implemented in practical systems with fast fading channels, since it requires a large overhead and complicated inter-cell coordination. Nevertheless, the results obtained provide a benchmark for possible performance for this joint procedure, and can give ideas for distributed ways to solve the optimization problem. That is, obtaining the same combination of capacity and fairness with a simplified version of the algorithm.

When scheduling users in a cellular network, there will always be a compromise between obtaining maximum capacity, and thereby the highest spectrum efficiency, and assuring maximum fairness for all users. Thus, during the planning we have to decide which parameter we want to optimize, knowing that it is not possible to obtain both at the same time.

Another idea is how noticeable the effect of using a fair algorithm is to the users. Perhaps more importantly, do the users actually have any interest in the fact that user

b's transfer rate is limited in order to give user a a minimum throughput, even though user b has superior channel conditions? In other words, there is a chance that users are greedy and only want the best possible rate at all times, not caring about other users in the same or neighbouring cells. Or we could look at the problem from a different angle by considering user satisfaction as the main criterium. Can we assume that users are satisfied if they get the data rate they pay for, independently of what other users get?

Chapter 7

Conclusions

7.1 Conclusions and contributions of this thesis

We have simulated joint user scheduling and power allocation for hexagonal cellular networks in order to analyze the relationship between system capacity, power allocation, and user selection. Traditional scheduling algorithms and a proposed multi-cell extension to the proportional fair scheduling have been tested together with binary power allocation, and their performances have been studied.

The two major findings presented in this report can be summarized as follows. First, increasing the minimum transmit power level, $P_{\min}$, for binary power allocation drastically reduces the obtained gain in system capacity. For the considered simulation parameters, we observe a significant reduction in the capacity gain when going from $P_{\min} = 0$ to $P_{\min} > 0$. Thus, the way to improve fairness seemingly has to go through scheduling of users, and not through an increase in $P_{\min}$.

Furthermore, the extension of proportional fair scheduling to a multi-cell network gives rates close to those obtained by maximum capacity scheduling. The difference between the two algorithms is controlled by the time horizon, which adjusts the compromise made between system capacity and fair distribution of resources. Even though the high complexity of the algorithm might be an obstacle because of the number of degrees of freedom, it is interesting as a benchmark for performance and it gives new insight into the optimization problem.

7.2 Suggestions for further research

For further research on the topic, the work could follow one or several of the proposed paths. The most interesting is to improve the performance of the V-PFS algorithm by lowering its complexity by finding a distributed alternative to the centralized algorithm. This would open for a feasible implementation with each cell acting on its own without the need for a central unit taking care of the coordination.

Secondly, the proposed algorithm, as well as new distributed versions, could be tested in a larger cellular network. That is, simulating more realistic networks with $N = 19$ or

even bigger, in order to see to which extent the algorithm is affected by interference and how many of the neighbouring cells have to be considered. An alternative is to adopt the technique of cell wrapping, which could give similar results.

Thirdly, the environment in which the V-PFS is tested could be modified to see if it still shows promising performances in other path loss, shadowing and multipath fading environments. In other words, this can give us insight into if the algorithm does perform as well for networks with non-homogenuous cell structure and channel characteristics.

Finally, the effects of the increase in $P_{\min}$ and using the scheduling algorithms in this report could be quantified through calculating JFI or another suitable measure of fairness. This would increase the knowledge on the effects of binary power allocation when it comes to fair distribution of resources.

Bibliography

[1] COST Action 231. Digital mobile radio towards future generation systems, final report. Technical report, COST Telecom, 1999.

[2] David Gesbert, Mohamed-Slim Alouini. Selective multi-user diversity. In *Proc. IEEE 3rd International Symposium on Signal Processing and Information Theory*, pages 162–165, Darmstadt, Germany, Dec. 2003.

[3] Mung Chiang. Geometric programming for communication systems. *Foundations and Trends in Communications and Information Theory*, 2(1/2):1–154, 2005.

[4] Hans Jørgen Bang, Torbjörn Ekman, David Gesbert. A channel predictive proportional fair scheduling algorithm. In *Proc. IEEE 6th Workshop on Signal Processing Advances in Wireless Communications*, pages 620–624, New York City, NY, USA, June 2005.

[5] Marios Kountouris, David Gesbert. Memory based opportunistic multi-user beamforming. In *Proc. IEEE International Symposium on Information Theory*, pages 1426–1430, Adelaide, Australia, Sept. 2005.

[6] Anders Gjendemsjø. *Simulating Wireless Communications* α-version. Tutorial on simulations for wireless communications.

[7] Andrea Goldsmith. *Wireless communications*. Cambridge University Press, 2005.

[8] Hoon Kim, Youngnam Han. A proportional fair scheduling for multicarrier transmission systems. *IEEE Communication Letters*, 9(3):210–212, March 2005.

[9] Vegard Hassel. *Design Issues and Performance Analysis for Opportunistic Scheduling Algorithms in Wireless Networks*. PhD thesis, Norwegian University of Science and Technology, NTNU, 2007.

[10] Stephen P. Boyd, Seung J. Kim, Lieven Vandenberghe, Arash Hassibi. A tutorial on geometric programming. *Optimization and Engineering*, 8(1):67–127, 2007.

[11] Rajendra K. Jain, Dah-Ming W. Chiu, William R. Hawe. A quantitative measure of fairness and discrimintation for resource allocation in shared computer systems. Technical report, Digital Equipment Corporation, Hudson, MA, USA, Sept. 1984.

[12] Jack M. Holtzman. Asymptotic analysis of proportional fair algorithm. In *Proc. IEEE 12th International Symposium on Personal, Indoor and Mobile Radio Communications*, pages F–33–F–37, San Diego, CA, USA, Sept 2001.

[13] Raymond Knopp, Pierre A. Humblet. Information capacity and power control in single-cell multiuser communications. In *Proc. IEEE International Conference on Communications*, pages 331–335, Seattle, WA, USA, June 1995.

[14] Masoud Ebrahimi, Mohammad A. Maddah-Ali, Amir K. Khadani. Throughput scaling in decentralized single-hop wireless networks with fading channels. Technical report, Electrical and Computer Engineering Departement, University of Waterloo, Waterloo, Canada, Aug. 2006.

[15] Jan E. Kirkebø, David Gesbert, Saad G. Kiani. Maximizing the capacity of wireless networks using multi-cell access schemes. In *Proc. IEEE 7th Workshop on Signal Processing Advances in Wireless Communications*, pages 1–5, Cannes, France, July 2006.

[16] Jean-Paul M.G. Linnartz. Wireless communication reference website, 2004. Available at `http://wireless.per.nl/`.

[17] Tian Bu, Li Li, Ramachandran Ramjee. Generalized proportional fair scheduling in third generation wireless data networks. In *Proc. IEEE 25th International Conference on Computer Communications*, pages 1–12, Barcelona, Spain, April 2006.

[18] Xin Liu, Edwin K. P. Chong, Ness B. Shroff. Joint scheduling and power-allocation for interference management in wireless networks. In *Proc. IEEE 56th Vehicular Technology Conference*, pages 1892–1896, Vancouver, Canada, Sept. 2002.

[19] Thomas M. Cover, Joy A. Thomas. *Elements of Information Theory.* John Wiley & Sons, 2nd edition, 2006.

[20] David Tse. Smart scheduling and dumb antennas, Sept. 2002. Presentation at Berkeley Wireless Research Center.

[21] David Gesbert, Saad G. Kiani, Anders Gjendemsjø, Geir E. Øien. Adaptation, coordination and distributed resource allocation in interference-limited wireless networks. To appear in the Proceedings of the IEEE (invited paper), Oct. 2007.

[22] Saad G. Kiani, Geir E. Øien, David Gesbert. Maximizing multicell capacity using distributed power allocation and scheduling. In *Proc. IEEE Wireless Communications and Networking Conference*, pages 1690–1694, Hong Kong, China, March 2007.

[23] Vegard Hassel, Geir E. Øien, Marius R. Hanssen. Spectral efficiency and fairness for opportunistic scheduling algorithms. *Submitted to IEEE Transactions on Wireless Communications*, 2007.

[24] Anders Gjendemsjø, David Gesbert, Geir E. Øien, Saad G. Kiani. Optimal power allocation and scheduling for two-cell capacity maximization. In *Proc. IEEE 4th International Symposium on Modeling and Optimization in Mobile, Ad Hoc and Wireless Networks*, pages 1–6, Boston, MA, USA, April 2006.

[25] Anders Gjendemsjø, David Gesbert, Geir E. Øien, Saad G. Kiani. Binary power control for multi-cell capacity maximization. In revision for IEEE Transactions on Wireless Communications, 2007.

Appendix A

Additional simulation results

This chapter contains results for additional simulations defined by the four scenarios in Chapter 4.2, but not presented in Chapter 5. The simulations are divided in two; the first part covers the investigation of binary power allocation and its performance with different levels for the minimum transmit power level. The second part presents results for different scheduling algorithms and their characteristics in two-cell hexagonal networks.

A.1 Binary power allocation with variable $P_{\mathbf{min}}$

A.1.1 Multi-cell case

We consider an increased cell radius r of 5000 m, and figures A.1, A.2, and A.3 basically show the same trends as for $r = 1000$ m documented in Chapter 5.1.3, but with a lower loss in capacity gain when increasing $P_{\min}$. Thus, the difference between using on/off and binary power allocation becomes smaller when cell radius increases.

# Cells	$P_{min} = 0$	$P_{min} = 0.1$	$P_{min} = 0.2$	$P_{min} = 0.3$
2	52.90 %	53.33 %	53.50 %	53.60 %
3	38.67 %	52.15 %	52.67 %	52.80 %
4	35.89 %	50.72 %	51.11 %	51.30 %
5	35.86 %	49.63 %	50.33 %	50.72 %
6	36.50 %	48.79 %	49.50 %	49.90 %
7	35.86 %	47.40 %	48.21 %	48.76 %

Table A.1: Percentage of cells emitting with $P_{\max}$ for $r = 5000$ m

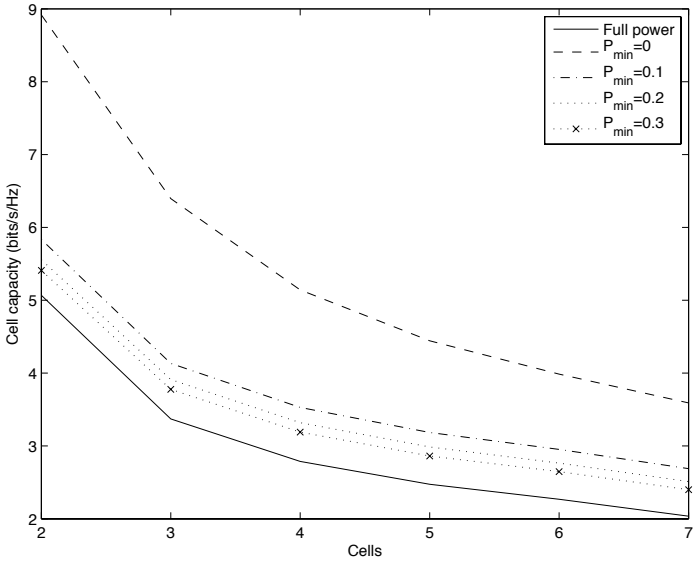

Figure A.1: Cell capacity vs. cells for $r = 5000$ m and variable $P_{\min}$

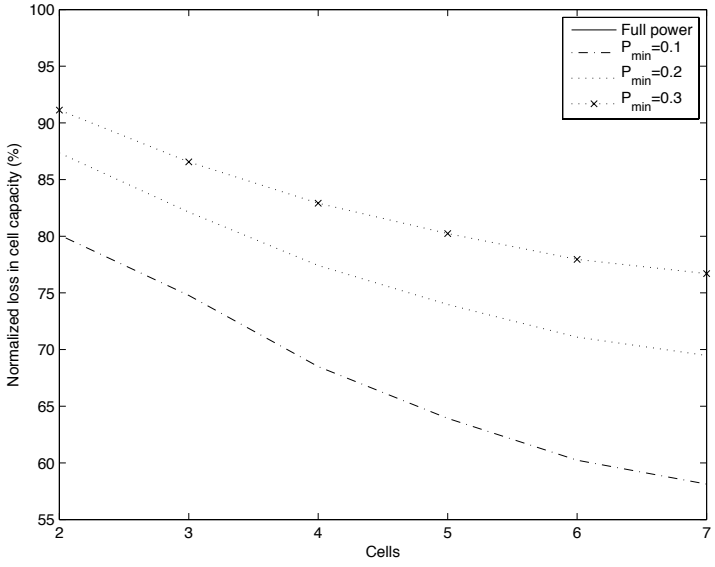

Figure A.2: Normalized capacity loss vs. cells for $r = 5000$ m and variable $P_{\min}$

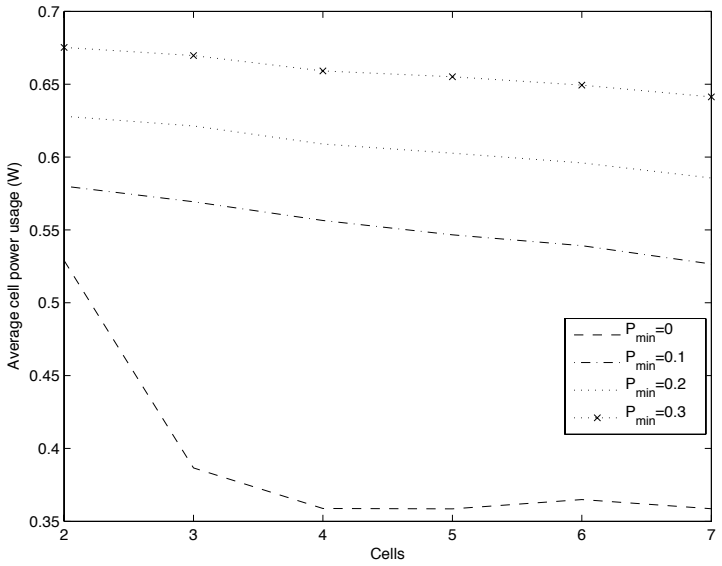

Figure A.3: Average power vs. cells for $r = 5000$ m and variable $P_{\min}$

A.2 Joint scheduling and power allocation performance

A.2.1 On/off power allocation

Cell radius $r = 1000$ m

Figures A.4 and A.5 show that for an increase in the value of i_c, the V-PFS and Max-Cap algorithms have close to equal average throughput. This is as expected, since an increase in i_c means a longer time horizon for the algorithm, and less stringent requirements for fairness.

Figures A.6, A.7, A.8, A.9, A.10, and A.11 show the distribution of users and rates for the Max-Cap-P, V-PFS, and V-PFS-P algorithms, respectively. We note the similar performance of Max-Cap-P and V-PFS-P when it comes to system capacity, as already mentioned in Chapter 5.2.1. V-PFS-P and Max-Cap have a rather spread out distribution of its user rates due to the power allocation, whereas V-PFS has a compact distribution of users and rates, since full power is employed.

Table A.2 illustrates the mean and variance overview for $r = 1000$ m, $i_c = 100$, and $P_{\min} = 0$. The pairs in the table are the mean and the variance of the rates for the different algorithms. We note the considerable difference in mean and variance between the algorithms. First, there is an important difference between having the possibility to adapt power levels, as explained earlier. Then, as the number of users increase the difference between V-PFS and Max-Cap becomes more visible, which is due to the fact that V-PFS maximizes the rate-average rate metric, wheras Max-Cap maximizes throughput.

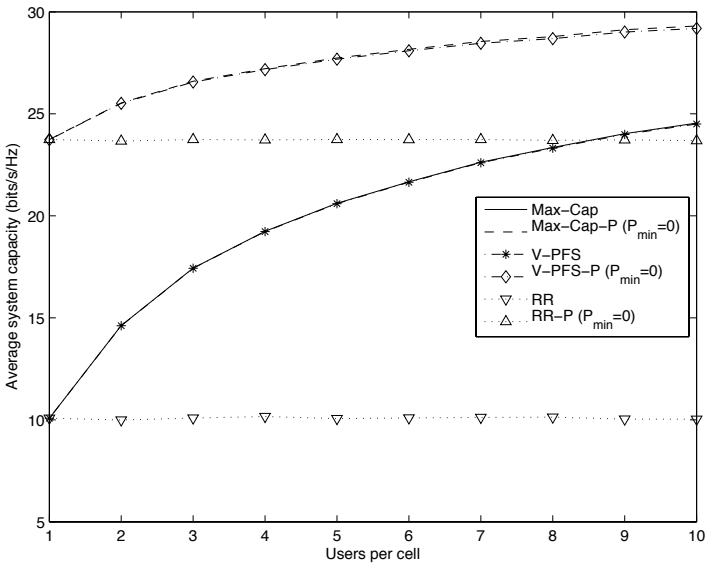

Figure A.4: Average system capacity vs. users for $r = 1000$ m, $i_c = 1000$, and $P_{\min} = 0$

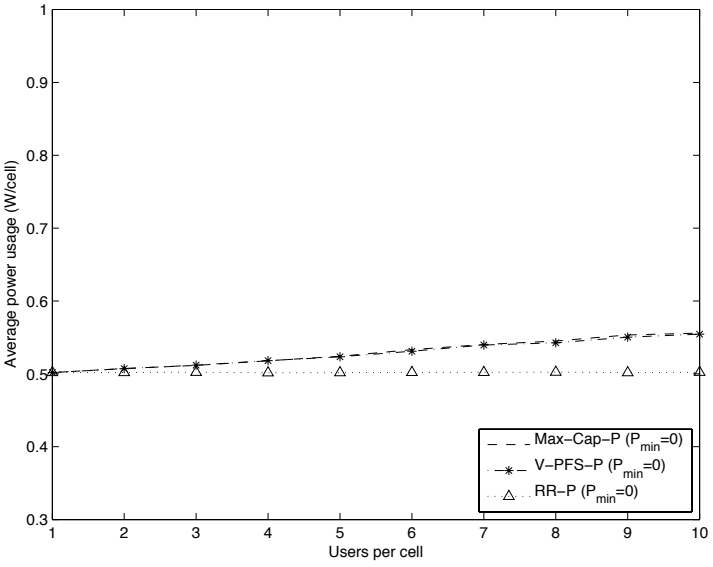

Figure A.5: Average power usage vs. users for $r = 1000$ m, $i_c = 1000$, and $P_{\min} = 0$

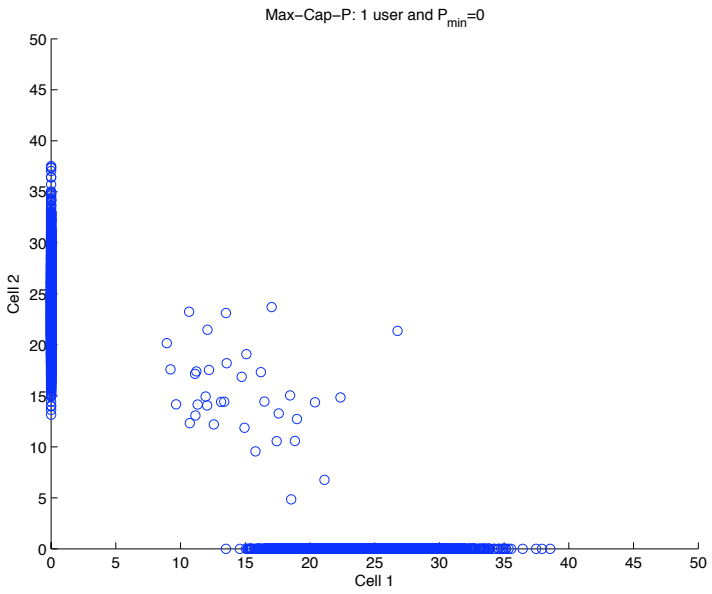

Figure A.6: 1 user scatter plot for Max-Cap with $r = 1000$ m, $i_c = 100$, and $P_{\min} = 0$

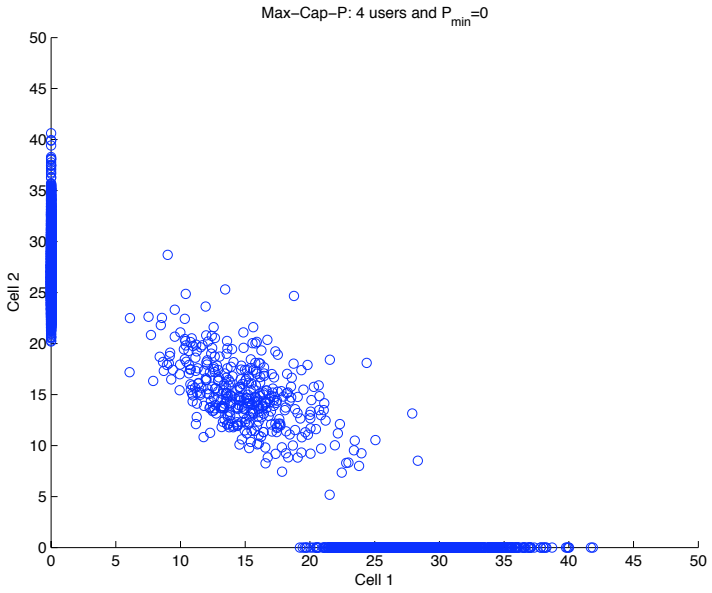

Figure A.7: 4 users scatter plot for Max-Cap with $r = 1000$ m, $i_c = 100$, and $P_{\min} = 0$

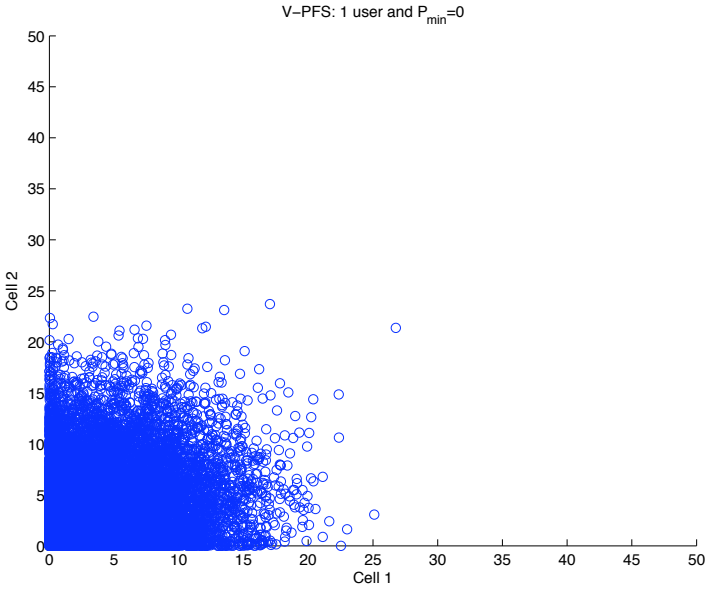

Figure A.8: 1 user scatter plot for V-PFS with $r = 1000$ m, $i_c = 100$, and $P_{\min} = 0$

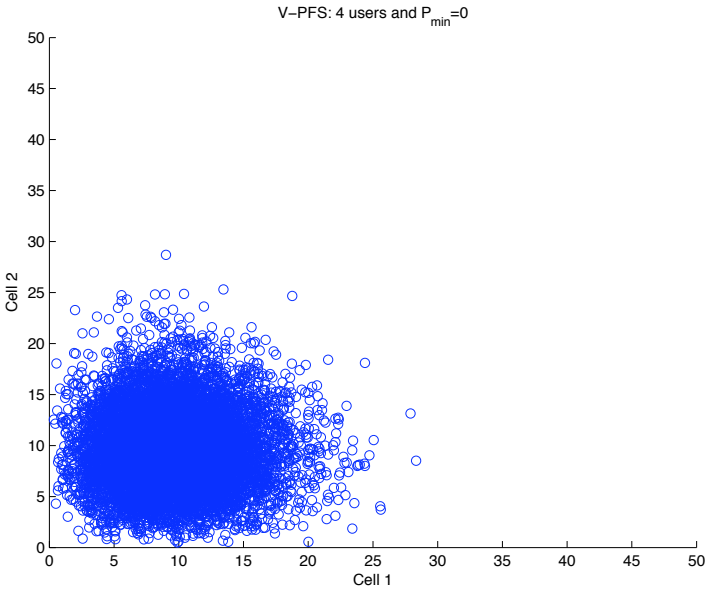

Figure A.9: 4 users scatter plot for V-PFS with $r = 1000$ m, $i_c = 100$, and $P_{\min} = 0$

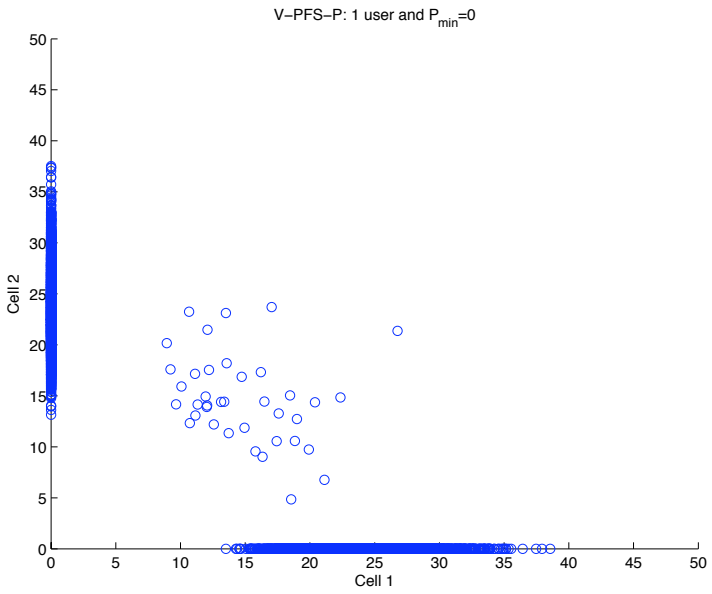

Figure A.10: 1 user scatter plot for V-PFS-P with $r = 1000$ m, $i_c = 100$, and $P_{\min} = 0$

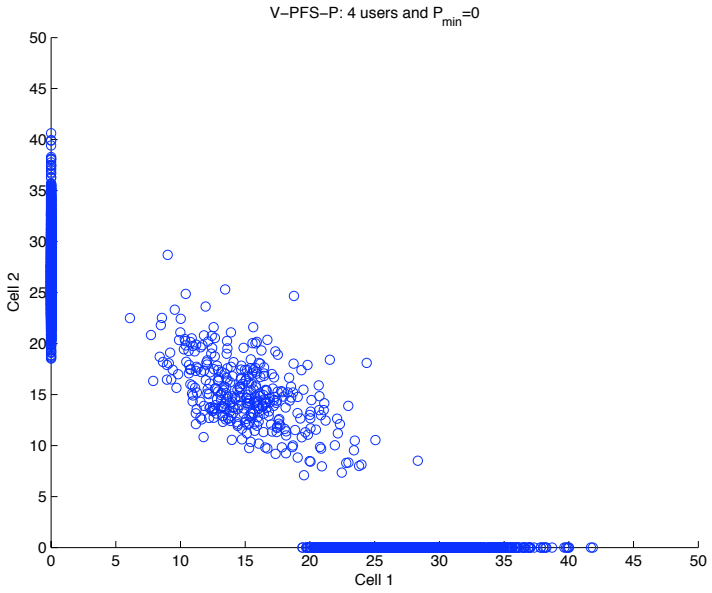

Figure A.11: 4 users scatter plot for V-PFS-P with $r = 1000$ m, $i_c = 100$, and $P_{\min} = 0$

The high variance for V-PFS-P and Max-Cap-P algorithms is due to the fact that they completely turn off cells, whereas V-PFS always gives throughput for both cells. This is easily observable from the scatter plots for user rates, where we observe that the rates for V-PFS are gathered in the same spot. For V-PFS-P and Max-Cap, the rates have a tendency to be distributed along the two axis, since the power control allows for the cells to be turned completely off.

# Users	*V-PFS*	*V-PFS-P*	*Max-Cap*
1	(5.04, 17.18)	(11.85, 145.13)	(11.87, 145.67)
4	(9.64, 13.65)	(13.43, 177.34)	(13.64, 181.75)
7	(11.14, 11.28)	(13.85, 182.57)	(14.23, 189.06)

Table A.2: Mean and variance overview for $r = 1000$ m, $i_c = 100$, and $P_{\min} = 0$

Cell radius $r = 5000$ m

Figures A.12 and A.14 show the average system capacity for RR, Max-Cap, and V-PFS scheduling algorithms for $i_c = 100$ and $i_c = 1000$, respectively. Figures A.13 and A.15 illustrate the power consumption for the three mentioned scheduling algorithms for the same two values of i_c, respectively.

We observe that fewer cells are turned off than for $r = 1000$ m, which can be explained by the fact that the LOS model makes it more interesting to turn off cells when r is small than when r is large, i.e., we have less interference.

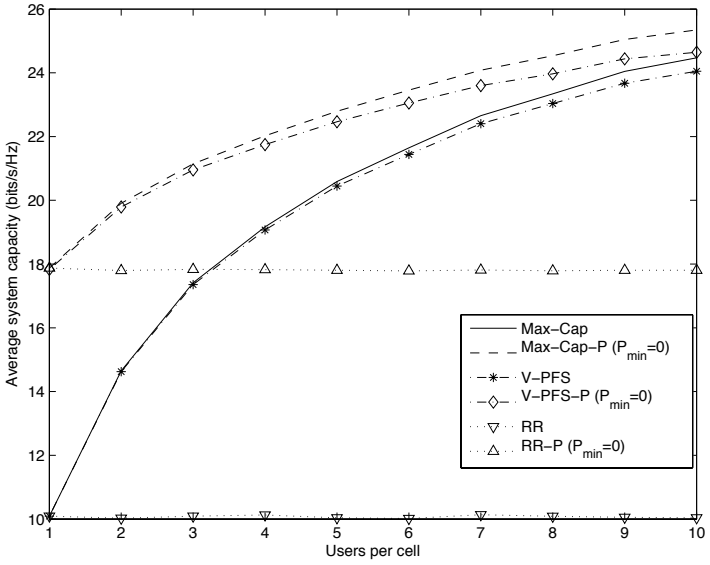

Figure A.12: Average system capacity vs. users for $r = 5000$ m, $i_c = 100$, and $P_{\min} = 0$

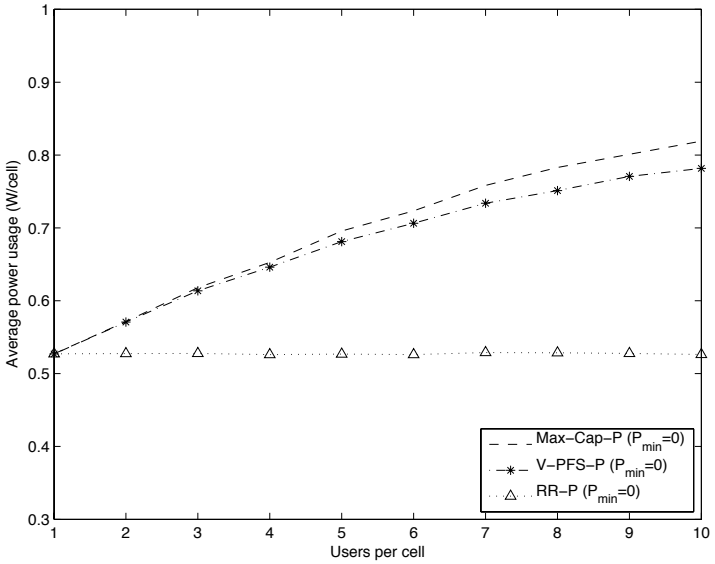

Figure A.13: Average power usage vs. users for $r = 5000$ m, $i_c = 100$, and $P_{\min} = 0$

A.2.2 Binary power allocation with variable $P_{\min}$

Cell radius $r = 1000$ m

Figures A.16 and A.17 show that for an increase in the value for i_c, the V-PFS and Max-Cap algorithms have the same average throughput. The trends observed are as expected, since a longer time window makes the two algorithms more similar given that the users experience the same average SNR.

Cell radius $r = 5000$ m

Figures A.18 and A.20 show the average system capacity for RR, Max-Cap, and V-PFS scheduling algorithms for $i_c = 100$ and $i_c = 1000$, respectively. Figures A.19 and A.21 illustrate the power consumption for the three mentioned scheduling algorithms for the same two values of i_c, respectively.

We note that for close to similar system capacity, V-PFS -P has a significantly lower power consumption than Max-Cap-P, meaning that more cells are turned off.

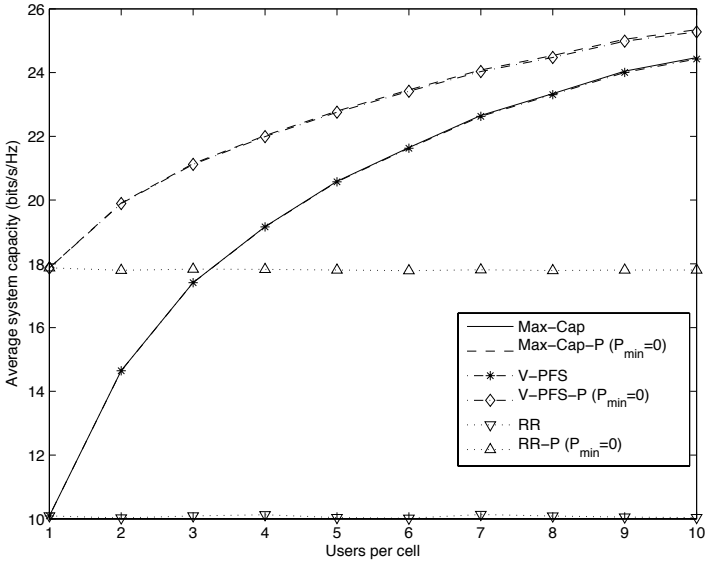

Figure A.14: Average system capacity vs. users for $r = 5000$ m, $i_c = 1000$, and $P_{\min} = 0$

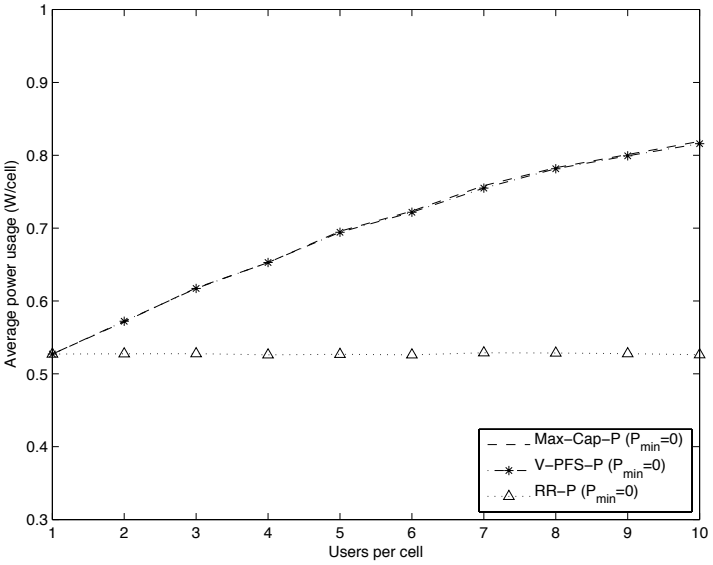

Figure A.15: Average power usage vs. users for $r = 5000$ m, $i_c = 1000$, and $P_{\min} = 0$

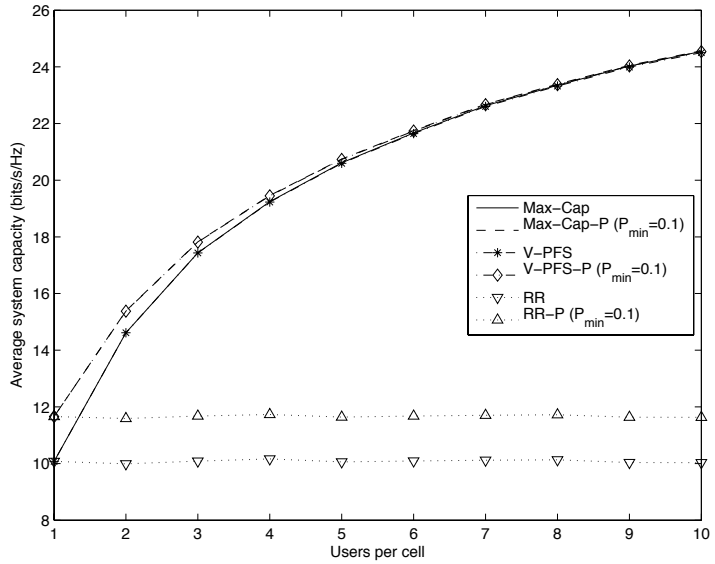

Figure A.16: Average system capacity vs. users for $r = 1000$ m, $i_c = 1000$, and $P_{\min} = 0.1$

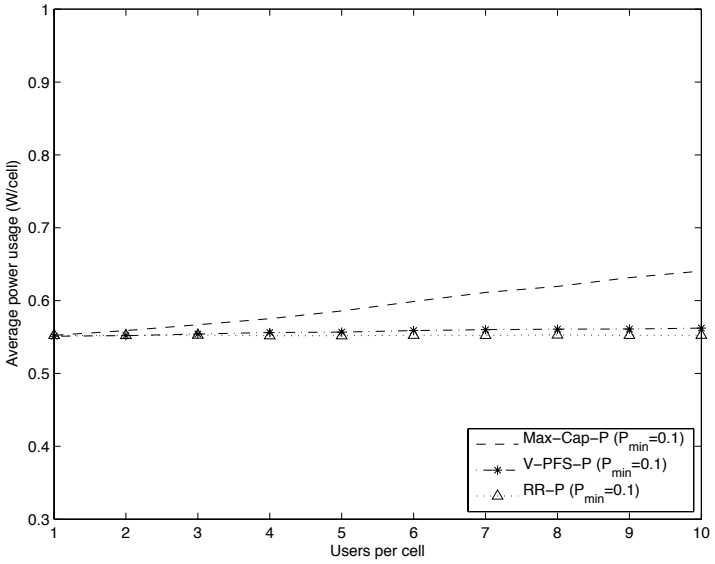

Figure A.17: Average power usage vs. users for $r = 1000$ m, $i_c = 1000$, and $P_{\min} = 0.1$

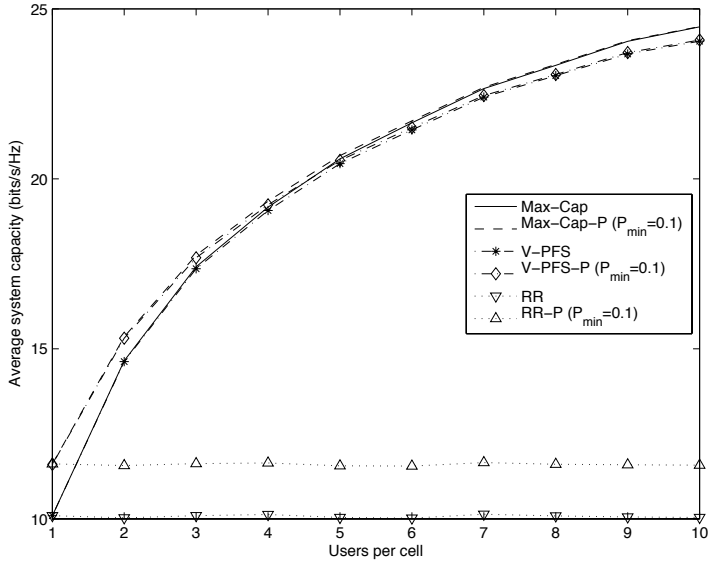

Figure A.18: Average system capacity vs. users for $r = 5000$ m, $i_c = 100$, and $P_{\min} = 0.1$

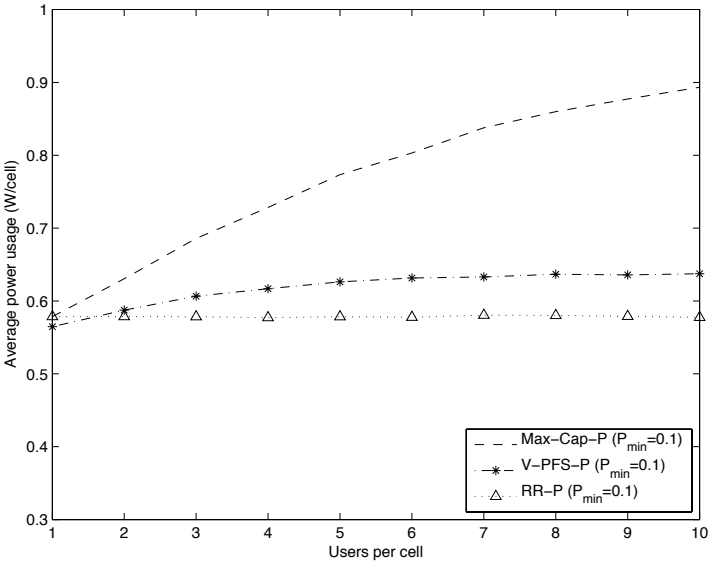

Figure A.19: Average power usage vs. users for $r = 5000$ m, $i_c = 100$, and $P_{\min} = 0.1$

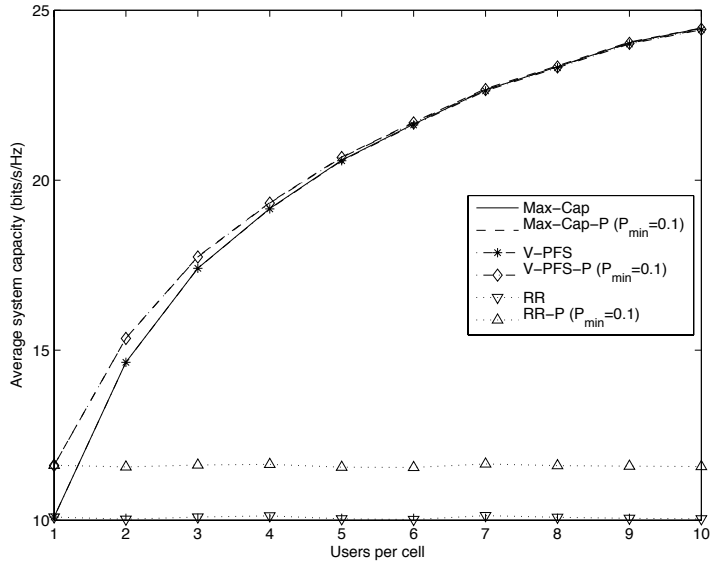

Figure A.20: Average system capacity vs. users for $r = 5000$ m, $i_c = 1000$, and $P_{\min} = 0.1$

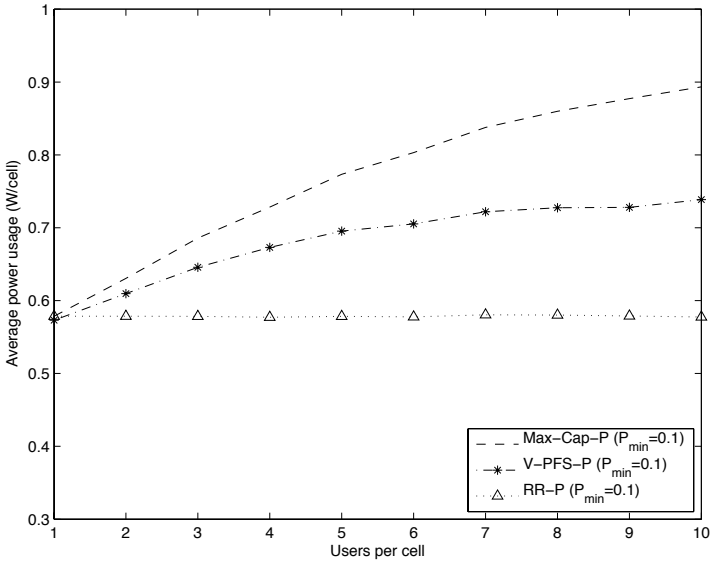

Figure A.21: Average power usage vs. users for $r = 5000$ m, $i_c = 1000$, and $P_{\min} = 0.1$